An OVERVIEW of Research and Development Activities in Machine Design and Drives

Prof. Baylon G. Fernandes

Department of Electrical Engineering,

Indian Institute of Technology Bombay

Flux Reversal Machine (FRM) for Rooftop Wind Energy Conversion

- ❑ Both windings and PMs are on stator
- ❑ Rotor has salient structure and no PMs or windings
- ❑ Rotor is simple and robust
- ❑ Conventional FRM → low winding factor of 0.5 due to concentrated winding
- ❑ Designed FRM → full pitch winding
  Improves winding factor to 1
- ❑ Prototype specs:
  - ➢ 6 stator poles with 4 magnets/pole
  - ➢ 14 rotor poles
  - ➢ 214 rpm, 50 Hz, 90 V, 20 A

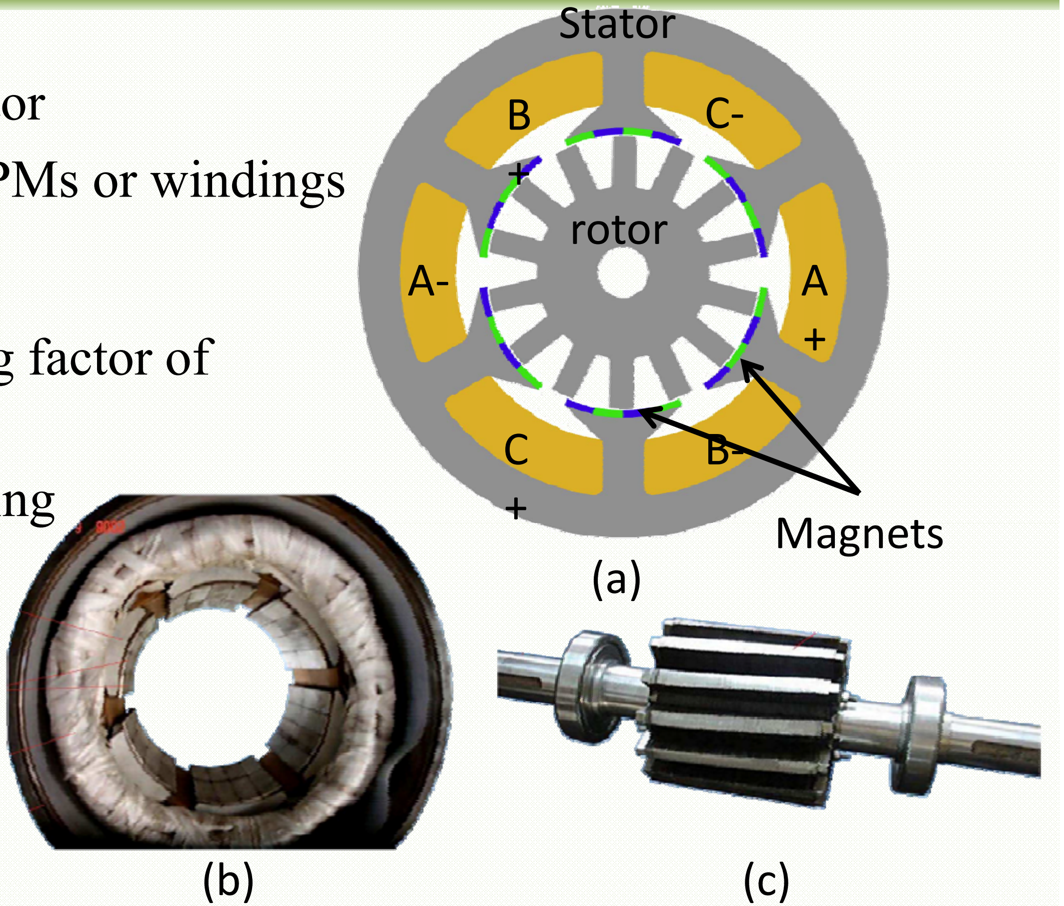

Fig. (a) FRM geometry, and its prototype (b) stator and (c) rotor

[1] D. S. More and B. G. Fernandes, "Modeling and Performance of Three Phase 6/14 Pole Flux Reversal Machine," IET Electric Power Applications, vol. 7, no. 2, pp. 131-139, Feb. 2013.

Slotless Permanent Magnet Generator for Wind Power Conversion

- ❑ Axial flux PM topology
  - ➢ high energy density
- ❑ Slot-less stator
  - ➢ no spiral laminations on stator (low cost)
- ❑ Dual rotor single stator with toroidal winding
  - ➢ lower copper loss
- ❑ Low speed design with 16 rotor poles
  - ➢ direct coupling with wind turbine
- ❑ Gear box is eliminated
  - ➢ high efficiency, lower cost

- ❑ Prototype specifications:

Power	1 kW
Voltage	230 V
Rotor poles	16

(a)

(b)

Fig. (a) Stator, (b) the two rotors.

High Torque Density Axial Flux PM Motor for Elevator Application

- ❑ Elevators require high torque, low speed motor
- ❑ Axial flux PM motor
  - → better utilization of available space
- ❑ Low speed motor
  - → high number of rotor poles
  - → improves specific torque
- ❑ Skewed stator slots
  - → reduced cogging torque

- ❑ Prototype specifications:

Power	12 kW @ 150 rpm
Torque	764 Nm
Slots / poles	72/24
Outer diameter	800 mm
Axial length	220 mm

(a)

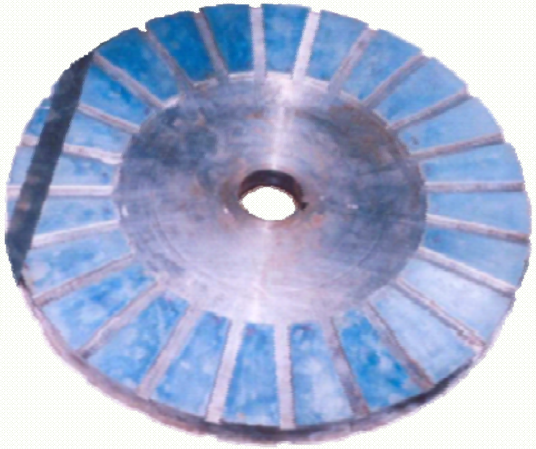

(b)

Fig. (a) Stator, and (b) Rotor.

High Speed Axial Flux Motor for Flywheel Energy Storage

- ❑ Axial flux topology → high energy density
- ❑ PM based motor → high efficiency (SmCo permanent magnets)
- ❑ High speed rotor: 24000 rpm
- ❑ Steel used: 40Ni2Cr1Mo28 → high rotor strength
- ❑ Dual stator, single rotor design

❑ Prototype specifications:

Power	4 kW @ 24,000 rpm
Stator slots	24
Rotor poles	8
Frequency	800 Hz

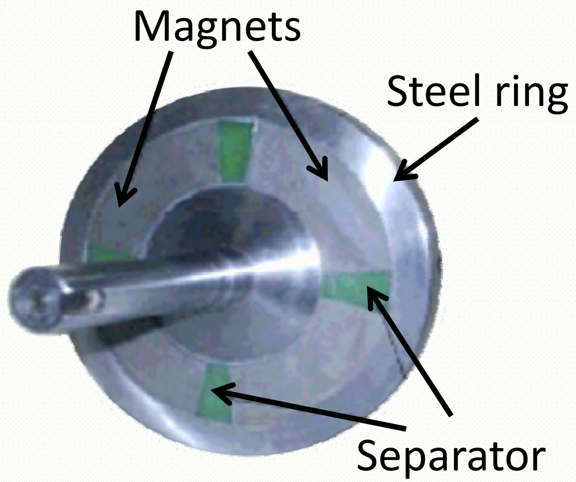

(a)

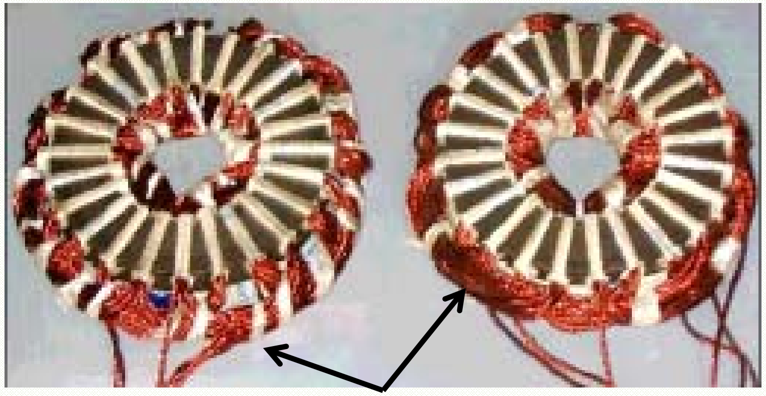

(b) The two stators

Fig. (a) Rotor and (b) stator geometry.

High Speed Axial Flux Motor for Centrifuge Application

- ❑ Axial flux topology → high speed application
- ❑ PM based motor→ high efficiency (PMs: SmCo)
- ❑ High speed rotor: 45,000 rpm, slotless stator
- ❑ Single stator, single rotor → should be able to run continuously for 20 years

- ❑ Prototype specifications

Power	94 W @ 45,000 rpm
Stator slots	12
Rotor poles	4
Outer diameter	140 mm
Length	50 mm

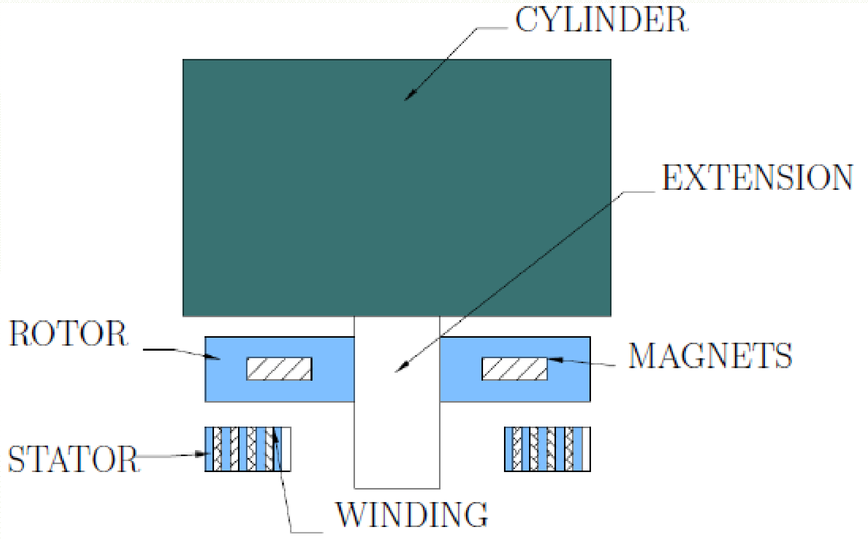

Fig. Cross-section view of the Axial flux motor.

High Speed Axial Flux Motor for Centrifuge Application

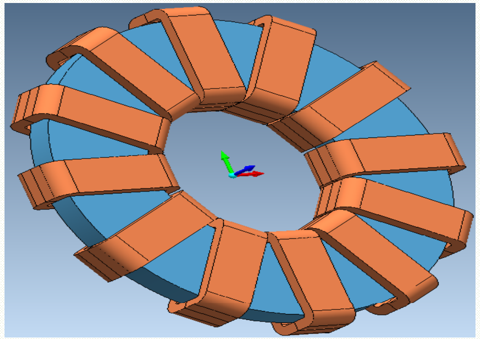

(a)

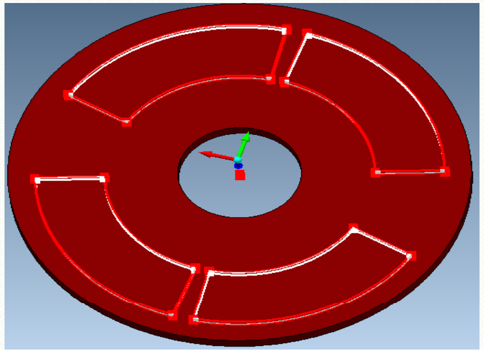

(b)

(c)

Fig. FEM models of the (a) stator and (b) rotor of the axial flux motor with magnetic core;
(c) Experimental prototype and
(d) Voltage and current waveforms measured at a speed of 20,000 rpm.

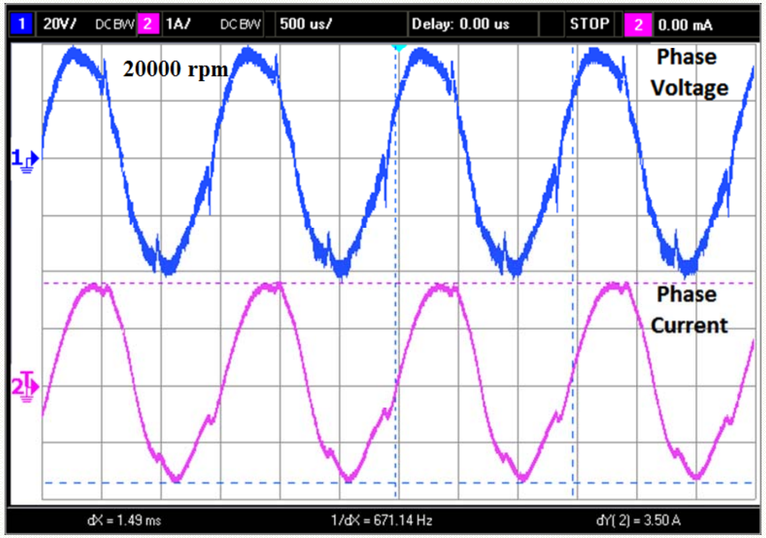

(d)

[1] S. Neethu, S. Pal, A. K. Wankhede and B. G. Fernandes, "High performance axial flux permanent magnet synchronous motor for high speed applications," *IECON 2017*, Beijing, 2017, pp. 5093-5098.

Coreless Axial Flux Permanent Magnet Motor with PCB Winding

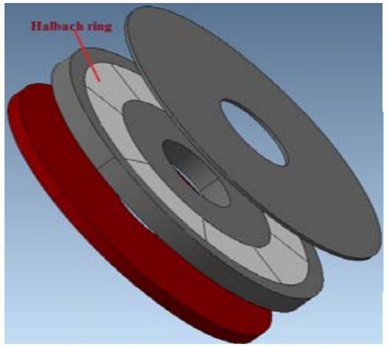

(a)

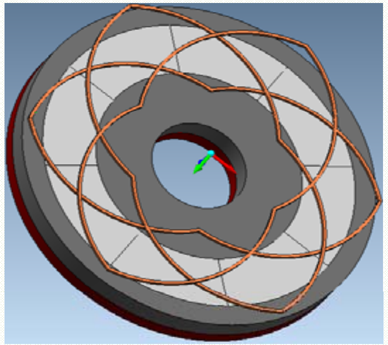

(b)

(c)

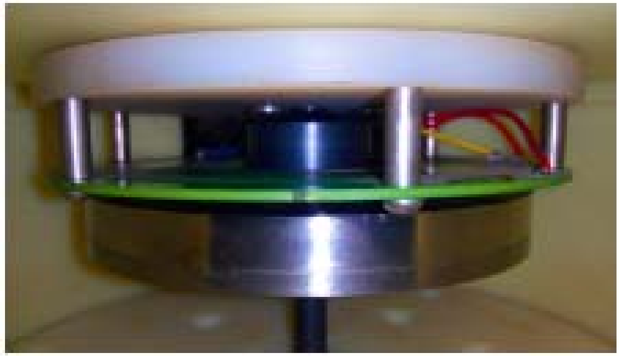

(d)

Fig. Coreless axial flux permanent magnet (AFPM) motor (a) Exploded view of the Hallbach rotor arrangement, and (b) Basic layout of the PCB winding;
Experimental prototype of AFPM
(c) Multilayer PCB stator,
(d) Motor assembly and (e) Measured waveforms at a speed of 24,000 rpm[1]

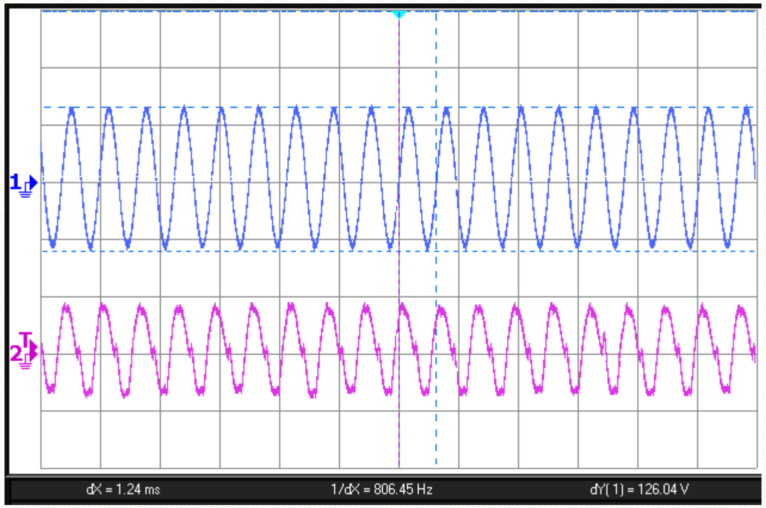

(e)

---

[1] N. S., S. P. Nikam, S. Singh, S. Pal, A. K. Wankhede and B. G. Fernandes, "High-Speed Coreless Axial Flux Permanent Magnet Motor with Printed Circuit Board Winding," in IEEE Transactions on Industry Applications.

Line-start Permanent Magnet Synchronous Motor for Irrigation Pumps

- ❑ Permanent magnet motor → higher efficiency
- ❑ Buried PMs are used with a squirrel cage for line start capability
- ❑ Line start capability → eliminates PE inverter → low cost

- ❑ Novel rotor geometry:
  - ❑ High flux concentration:
    → low cost ferrites can be used
  - ❑ High efficiency and specific power
  - ❑ Can synchronize at lower voltage
  - ❑ High power factor : 0.97

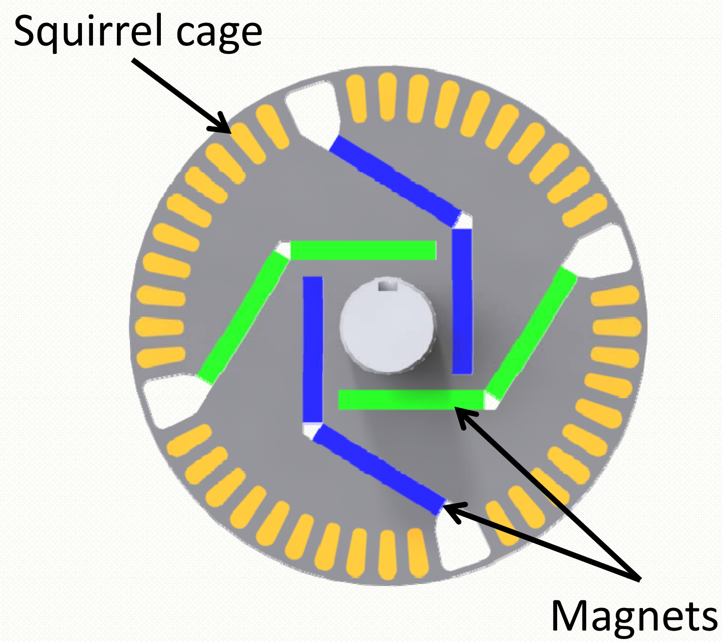

Fig. Rotor geometry.

An Energy Efficient Line-Start Two-Pole Ferrite Assisted SRM for Water Pumps

- ❑ High rotor saliency is achieved.
- ❑ Rotor cage is embedded in the reluctance path of the flux barriers → improves the starting characteristic and rotor synchronization.
- ❑ Improved motor efficiency is achieved → meets the new international efficiency (IE-4) standard for line-start application.[1]

Fig. Prototype of the ferrite assisted LS SyRM (a) finished rotor, (b)-(c) arc and rectangular ferrite magnets, (d) magnets placed in the rotor, (e) stator inside the frame, (f) star-connected distributed winding on the stator and (g) assembled motor.[1]

---

[1] S. Baka, S. Sashidhar and B. G. Fernandes, "Design of an Energy Efficient Line-Start Two-Pole Ferrite Assisted Synchronous Reluctance Motor for Water Pumps," in *IEEE Transactions on Energy Conversion*, vol. 36, no. 2, pp. 961-970, June 2021, doi: 10.1109/TEC.2020.3029110.

Low-Cost High Speed BLDC motor for PV Based Deep Bore-well Submersible Pump

- Problem:
  - Motor has to fit inside a 4-inch bore-well (100 mm) and should be submersible.
  - Motor has to be tubular (< D/L ratio).
  - High current density
  - High speed pump (2 hp, 2880 rpm)

- Solution:
  - Ferrite magnets → low cost
  - Spoke type rotor → flux concentration
  - Semi Modular Dual Stack rotor
  - Minimizes shaft flux leakage
  - Retains rotor integrity for high speed

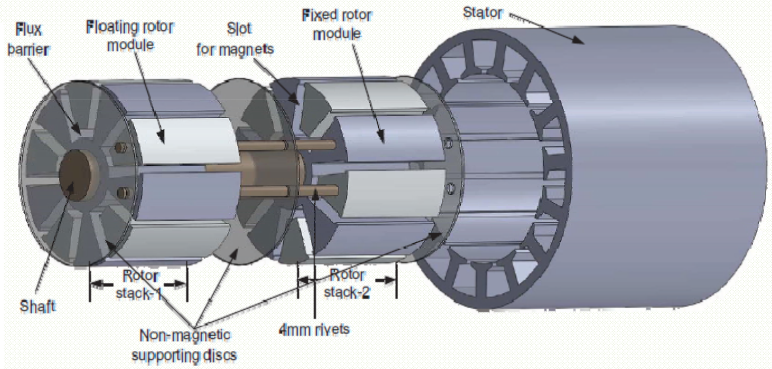

Fig. Submersible semi-modular dual stack spoke type BLDC motor

Fig. Hardware prototype [1].

[1] S. Sashidhar and B. G. Fernandes, "A Novel Ferrite SMDS Spoke-Type BLDC Motor for PV Bore-Well Submersible Water Pumps," in *IEEE Transactions on Industrial Electronics*, vol. 64, no. 1, pp. 104-114, Jan. 2017.

BLDC Motor and Controller for a 3 hp Solar Water (surface) Pump

- BLDC motor has 6 poles, 9 slots and is rated for 7 Nm of load torque at 3,000 RPM.
- Sensorless control is employed which reduces the component count.

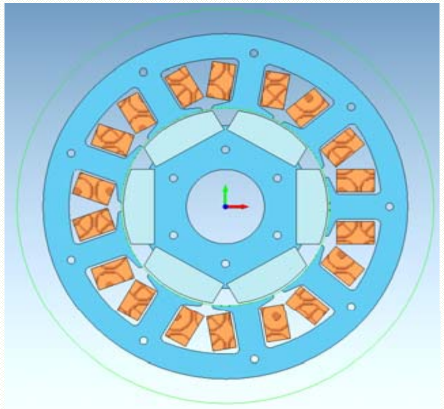

(a)

(b)

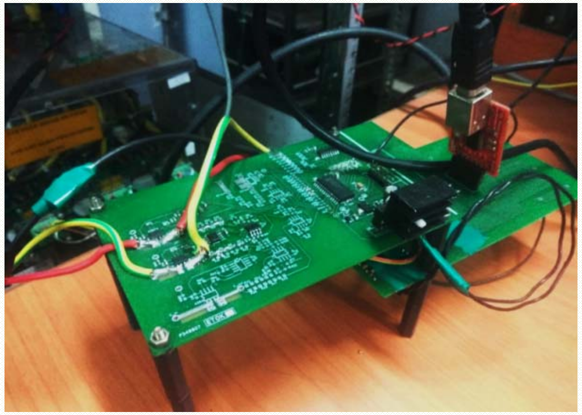

(c)

Fig. (a) FEA model of the BLDC motor, (b) Fabricated prototype of the BLDV motor is retrofitted with the Kirloskar pump, (c) The first generation PCB for drive interface and (d) the system architecture for integrating solar PV.

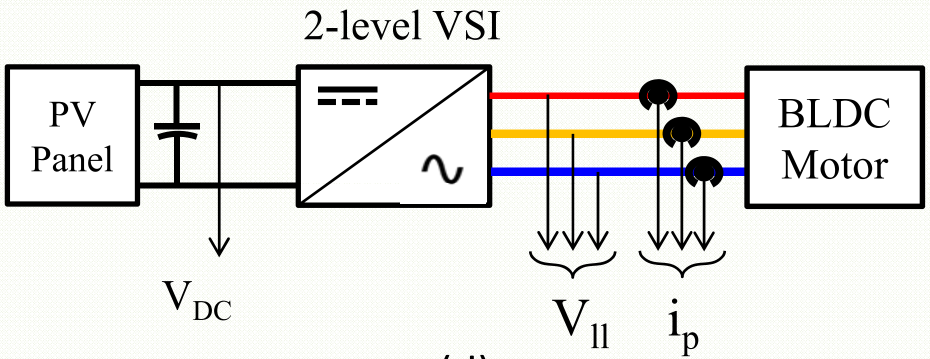

(d)

Toroidal Winding for Efficiency Improvement of a 5 hp Induction Machine

- Salient features of the Toroidal winding SCIM[1]
  - Wound around the stator back-iron.
  - High stator fill-factor (≈ 0.6).
  - Non-overlapping coils.
  - Simple coil winding leads to ease of manufacturing.
  - Aluminum is used as the rotor bar material.
- Conclusion: Toroidal winding helps improve efficiency in squirrel cage induction machine (SCIM).

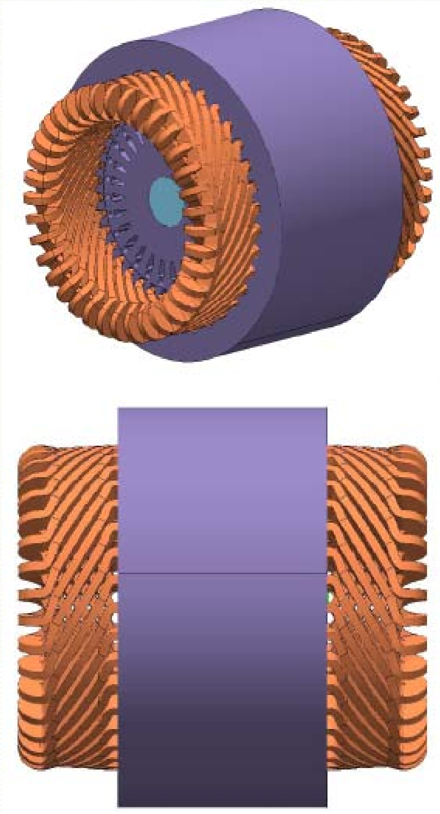

(a)

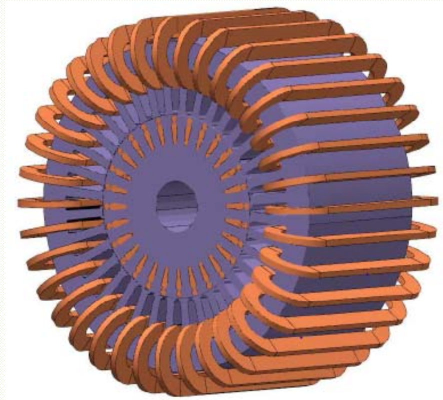

(b)

Fig. Comparative study between SCIM models with (a) distributed and (b) toroidal windings[1].

---

[1] S. Sashidhar, S. Mathew and B. G. Fernandes, "Novel Toroidal Winding for Efficiency Improvement of a Line-Start Induction Motor," *IECON 2018*, pp. 607-612, doi: 10.1109/IECON.2018.8591812.

Analyzing Rotor Bar Shape and Hybrid Rotor Structure for High-speed Induction Motor

- A novel rotor bar shape is proposed for a 630 W, 1,50,000 RPM laminated rotor induction motor (LRIM)[1], which
  - enhances the torque density of the motor by 13% and also satisfies the mechanical stress constraints.
- A novel rotor design is proposed suitable for high-speed spindle application,
  - with a high conducting material for the rotor bars and
  - a high strength alloy for the end rings to reduce stress levels in the rotor.

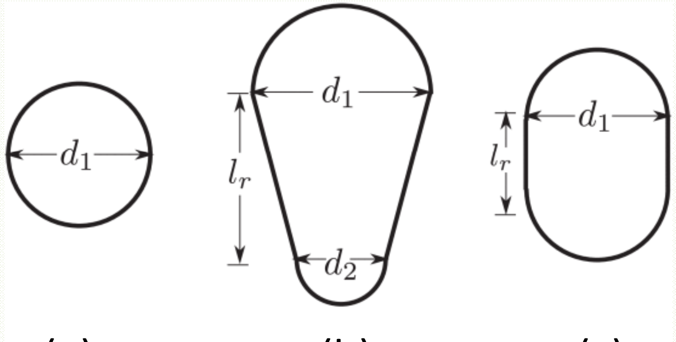

(a) (b) (c)

Fig. Different geometry of rotor bar of a LRIM[1] (a) circular shape, (b) drop bar shape and (c) modified drop bar shape.

[1] S. Mathew, R. M. Ram Kumar and B. G. Fernandes, "A novel rotor bar shape for enhancing the torque density of high-speed induction motor," ICEM 2020, pp. 2365-2371, doi: 10.1109/ICEM49940.2020.9270647.

[2] S. Mathew, R. M. R. Kumar, N. K. Endla, C. Vundru, R. Singh and B. G. Fernandes, "Development of a Hybrid Rotor Structure for high-speed Laminated Rotor Induction Motor," IEMDC 2021, pp. 1-7, doi: 10.1109/IEMDC47953.2021.9449519.

Improving Saliency of a High Speed SynRel Rotor Using High Strength Martensitic Sleeve

- A 3.5 kW, 60,000 RPM high speed synchronous reluctance (SynRel) machine is designed for an electric assist turbocharger (EAT) [1]. It discloses benefits of the proposed high strength martensitic sleeve rotor configuration such as
  - The optimized sleeve rotor produces 4.5% and 46.7% more torque than the SynRel machines using high and low strength laminations with conventional rotor configurations.
  - This is achieved with nearly 90% by volume of the conventional rotor lamination.

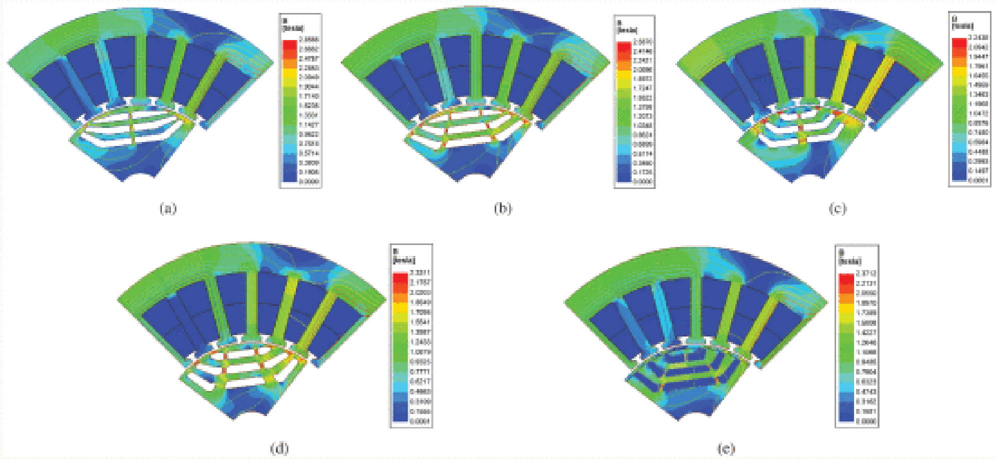

Fig. Flux density at rated condition for optimized SynRel configuration (a) HS centre rib (b) HS side rib (c) centre rib (d) side rib (e) sleeve rotor (proposed).

---

[1] R. M. Ram Kumar, G. Vakil, A. L. Rocca, D. Gerada, C. Gerada and B. G. Fernandes, "Improving the Saliency of a High Speed SynRel Rotor by using High Strength Martensitic Sleeve," *2021 International Conference on Sustainable Energy and Future Electric Transportation (SEFET)*, 2021, pp. 1-6, doi: 10.1109/SeFet48154.2021.9375705.

Switched Reluctance Motor for In-wheel Electric Motorcycle

- ❑ Switched reluctance motor
  → no permanent magnets → low cost
- ❑ Simple, robust construction, capable of operating at high temperatures
- ❑ Hub motor eliminates transmission
- ❑ Outer rotor configuration → higher torque density

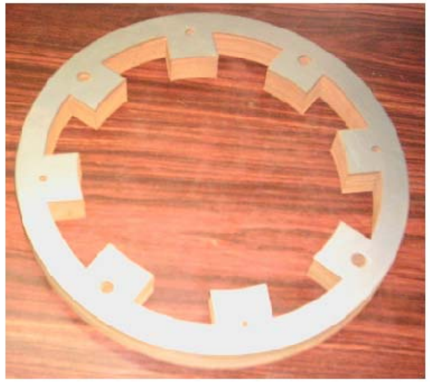

(a)

- ❑ Prototype specifications:

Power	3 kW
Rated rpm	1000
Stator/rotor poles	6/8
Outer diameter	290 mm
axial length	130 mm

(b)

(c)

Fig. (a) Rotor, (b) Stator laminations and (c) Stator winding.

Poly-phase Segmented Rotor SRM for Electric Vehicle

- Five phase 10/8 segmented rotor SRM[1]
  - → improves torque density
  - → improves constant power range
- Two phases conduct at a time
  - → higher torque output
  - → induces magnetic asymmetry in the motor.
- Bipolar excitation strategy
  - → eliminates magnetic asymmetry
  - → number of switches per phase remains the same (2)

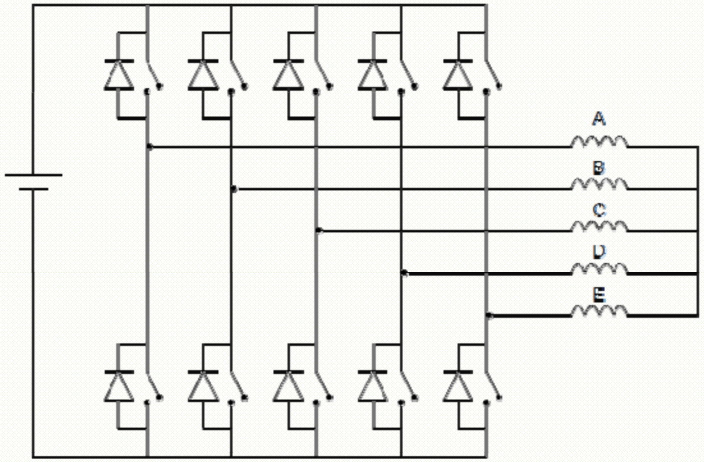

(a)

(b)

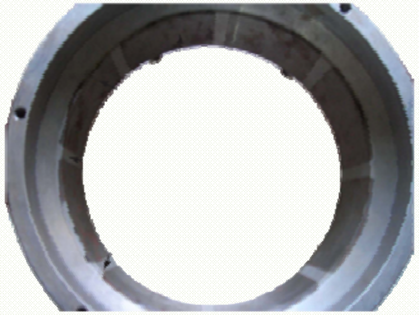

(c)

Fig. (a) 5-phase, bipolar SRM inverter, (b) Stator and (c) Rotor.

[1] R. Vandana, S. Nikam and B. G. Fernandes, "A High Torque Poly-phase Segmented Switched Reluctance Motor with Novel Excitation Strategy," IET Electric Power Applications, vol. 6, no. 7, pp. 375-384, Aug. 2012.

Concentrated Winding Segmented Rotor SRM for In-wheel EV

- ❑ Outer rotor, in-wheel SRM → Eliminates transmission and associated losses
- ❑ Low speed, high torque motor → Torque density must be improved

Salient features of the SRM:

- ❑ Segmented rotor SRM (SSRM)[1]
  - → high torque density
- ❑ SSRM employees full pitch winding
  - → high end winding copper loss and weight
- ❑ Thus concentrated winding SSRM is designed
  - → Alternate thick and thin stator poles
- ❑ Higher number of rotor segments
  - → Improves specific torque and efficiency

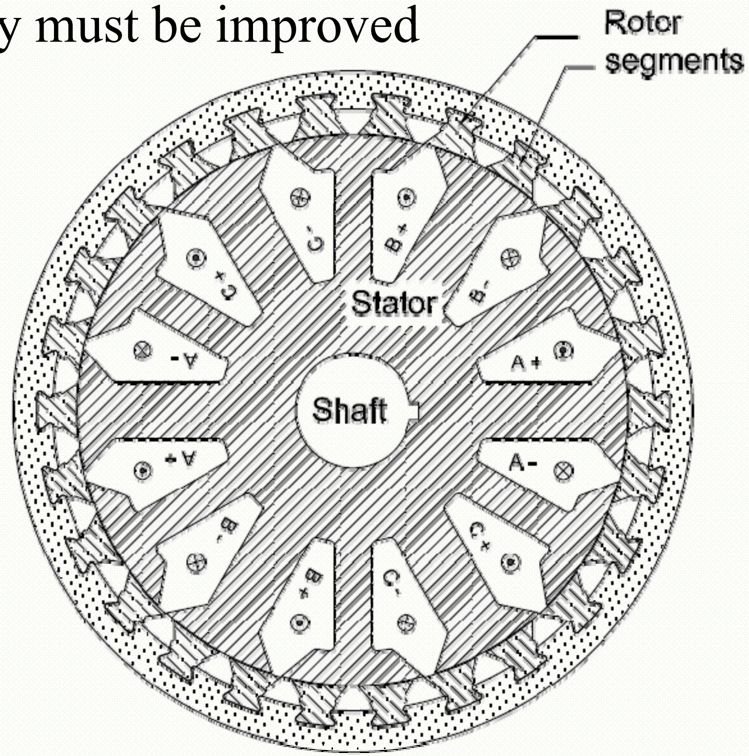

Fig. Geometry of the 12/26 segmented rotor SRM

[1] S. P. Nikam, V. Rallabandi and B. G. Fernandes, "A High-Torque-Density Permanent-Magnet Free Motor for in-Wheel Electric Vehicle Application," in *IEEE Transactions on Industry Applications*, vol. 48, no. 6, pp. 2287-2295, Nov.-Dec. 2012, doi: 10.1109/TIA.2012.2227053.

Concentrated Winding Segmented Rotor SRM for In-wheel EV

❑ Prototype specifications:

Torque	24 Nm @ 600 rpm
No. of Stator slots	12
No. of Rotor segments	26
Outer diameter	230 mm
Stack length	40 mm
Overall length	102 mm

Lamination stack

Shaft

Stator winding

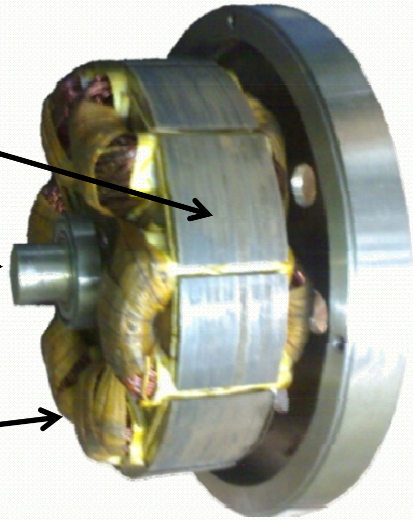

(a)

Rotor segments

Non magnetic support

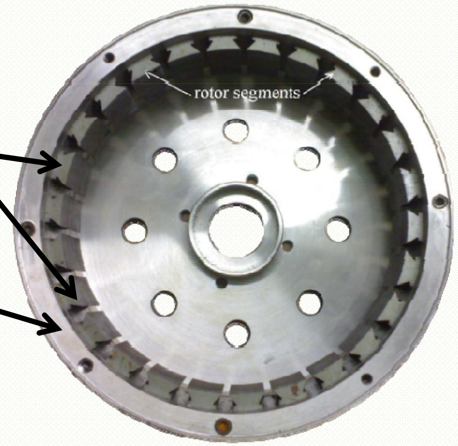

(b)

Fig. (a) Stator and (b) Rotor of the segmented rotor switch reluctance motor (SSRM)[2].

[2] V. R and B. G. Fernandes, "Design Methodology for High-Performance Segmented Rotor Switched Reluctance Motors," in *IEEE Transactions on Energy Conversion*, vol. 30, no. 1, pp. 11-21, March 2015.

Axial Flux Segmented Rotor Hub SRM for Electric Two Wheeler

- ❑ Axial flux motor → high torque density in large D/L ratio hub motor
- ❑ Three-phase, dual-rotor, single-stator configuration
- ❑ TORUS winding arrangement → lower copper loss
- ❑ Higher number of rotor poles than the stator slots → higher specific torque

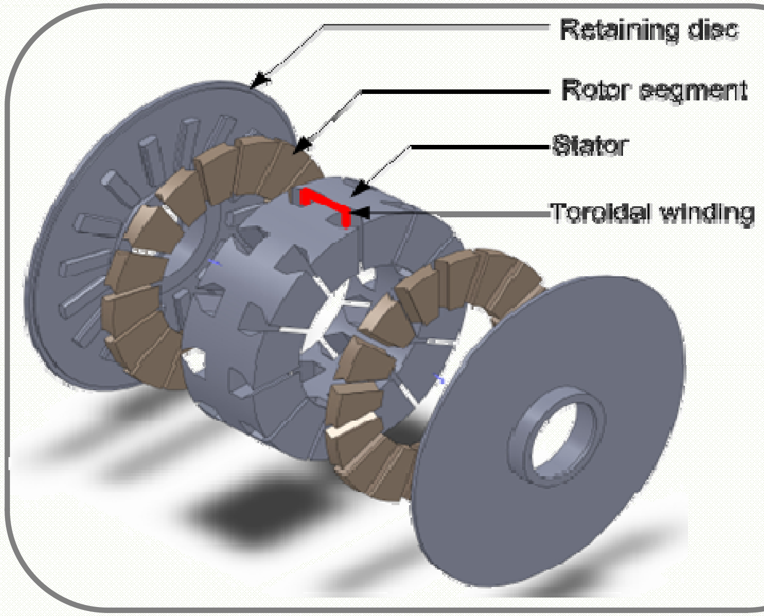

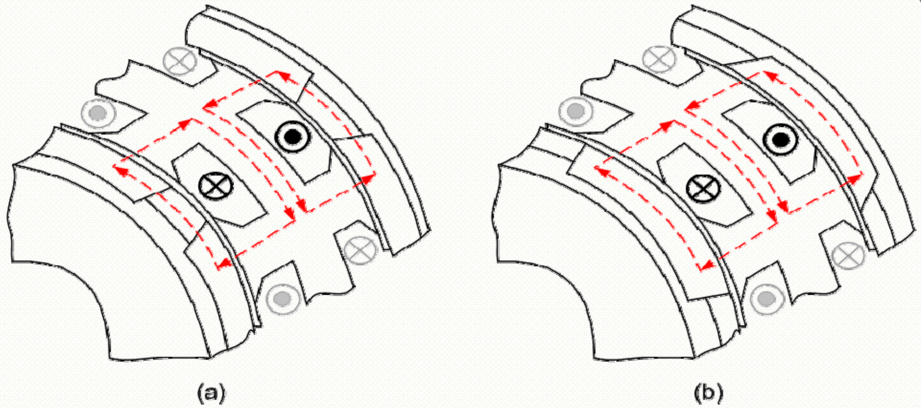

(a) Unaligned flux path, (b) Aligned flux path

(a) Conceptual geometry (b) SRM flux paths

[1] R. Madhavan and B. G. Fernandes, "Axial Flux Segmented SRM with a Higher Number of Rotor Segments for Electric Vehicles," IEEE Trans. on Energy Conversion, vol. 28, no. 1, pp. 203-213, March 2013.

Axial Flux Segmented Rotor Hub SRM for Electric Two Wheeler

Prototype specifications:

Rated power	1.5 kW at 600 rpm
Outer diameter	220 mm
Axial length	110 mm

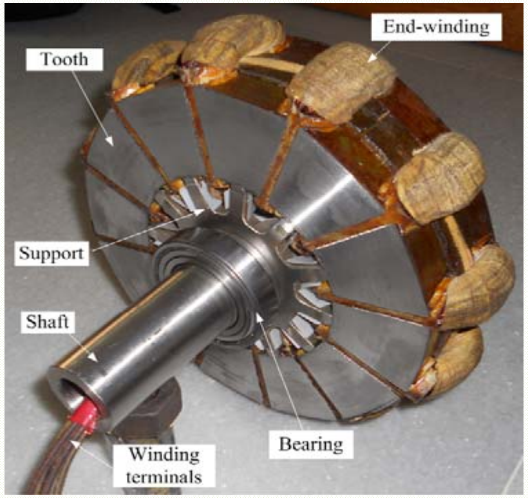

(a)

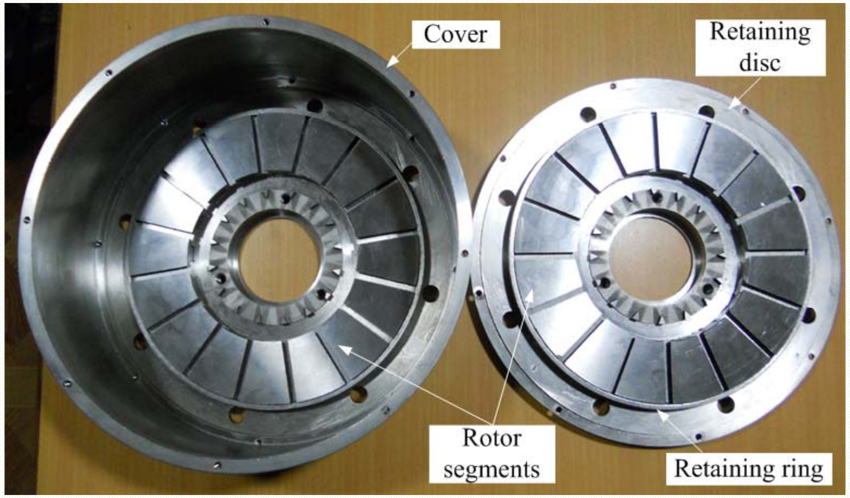

(b)

Fig. (a) Stator and (b) Two rotors of the fabricated motor.

[2] R. Madhavan and B. G. Fernandes, "Performance Improvement in Axial Flux Segmented Rotor Switched Reluctance Motor," IEEE Trans. on Energy Conversion, vol. 29, no. 3, pp. 641-651, Sept. 2014.

Ferrite Based Permanent Magnet Motor for Electric-Assist Campus Bicycle

- 250W permanent magnet motor for Electric Assist Bicycle
- Ferrite magnets → Low cost solution
- Planetary gear → High torque capability, compact design
- High efficiency

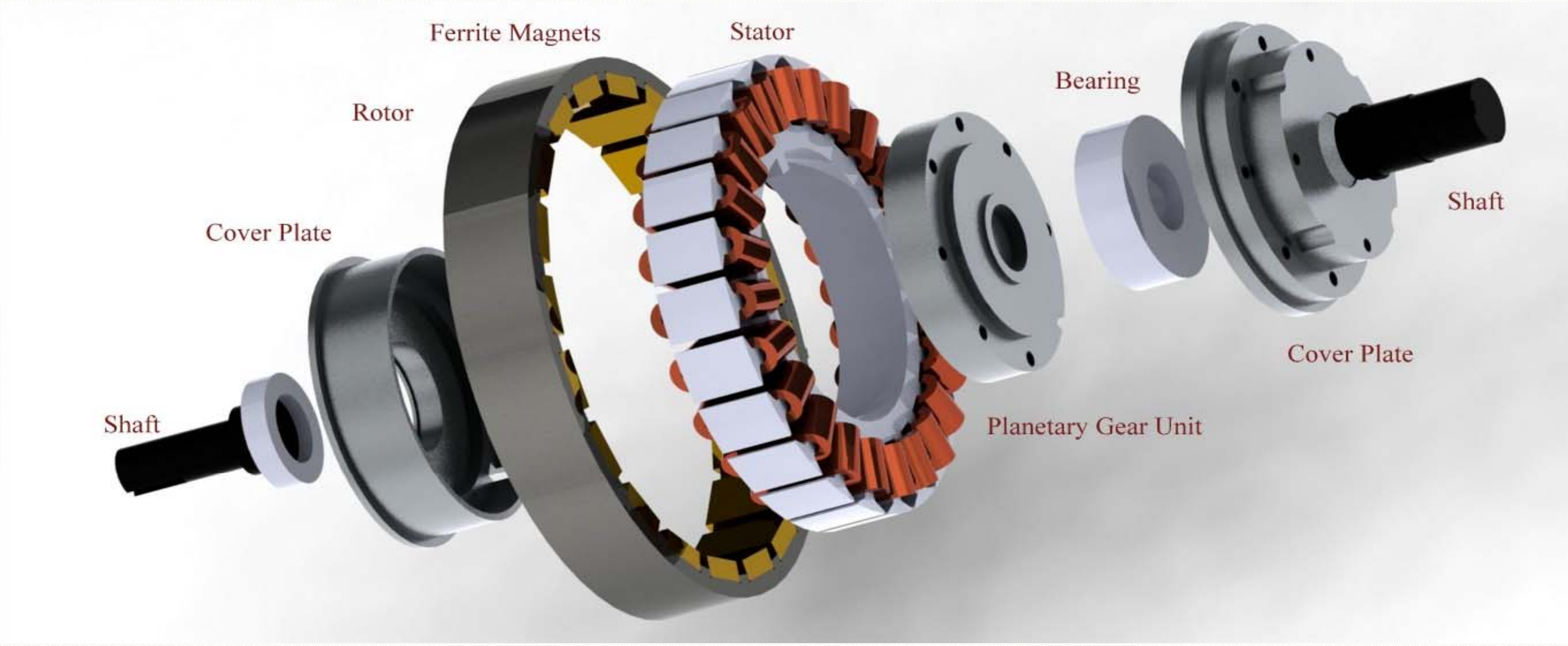

Ferrite Based Permanent Magnet Motor For Electric-Assist Campus Bicycle

- The developed prototype complete with the motor controller and battery.

High Efficiency Switched Reluctance Motor Based Ceiling Fan

- ❑ Ceiling fan is one of the most inefficient electrical appliances.
- ❑ Uses single phase induction motor
  - ➢ low cost, rugged but typical efficiency: 15 to 30% only
- ❑ The IM is replaced with SRM.
  - ➢ no permanent magnets / copper bars on rotor
  - ➢ robust, low cost

Salient features of the SRM:

- ❑ Two phase design: 4 stator poles (coils)
  - ➢ low power electronic device count
- ❑ Multiple teeth (4) per stator pole
  - ➢ magnetic gearing effect: torque amplification
  - ➢ lower copper loss
- ❑ High number of rotor poles (18)
  - ➢ 16/18 pole SRM
  - ➢ higher specific torque

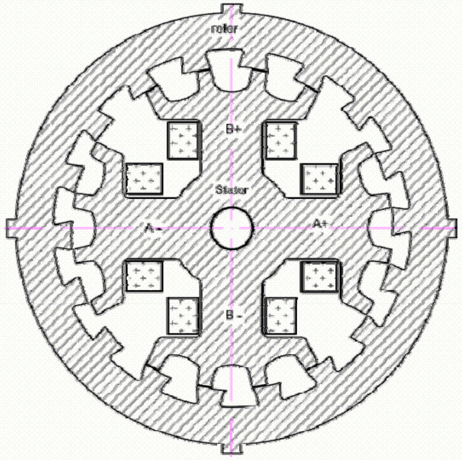

(a)

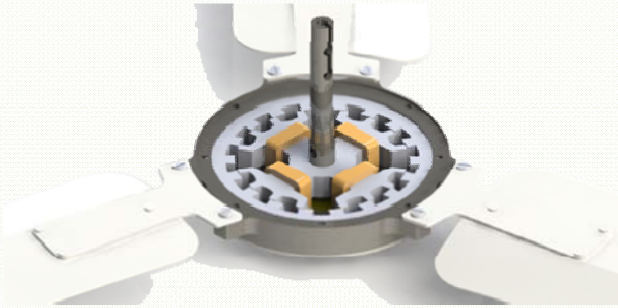

(b)

Fig. (a) SRM geometry and (b) SRM based ceiling fan

High Efficiency Switched Reluctance Motor Based Ceiling Fan

- ❑The SRM is driven using a C-dump converter
  - → single switch and single diode per phase
  - → lower cost
- ❑The SRM consumes 42 Watt power at rated rpm and with same blades as compared to 73 Watt of the IM.

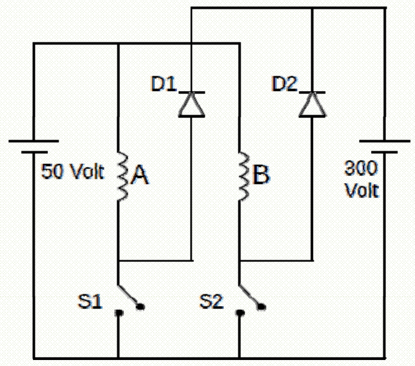

(a)

(b)

(c)

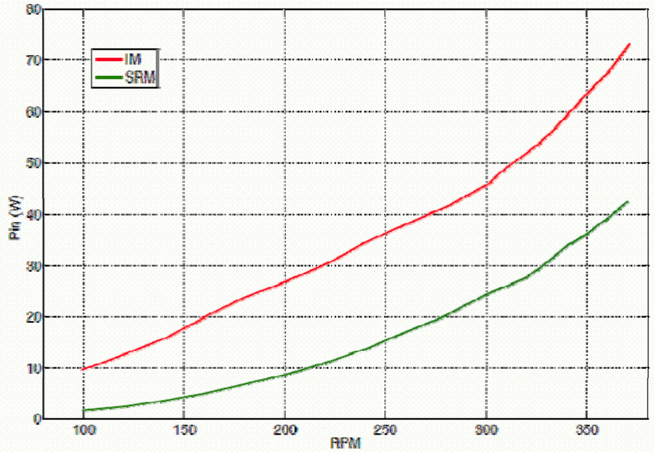

(d)

Fig. (a) C-dump converter, (b)-(c) Rotor and stator of the SRM motor, (d) Comparison of the power intake of IM and SRM based fans.

Low Cost Ferrite BLDC Motor based DC Mixer Grinder for DC Micro-grids

- ❑ Operates on DC: ideal for renewable sources, DC grids
- ❑ BLDC motor: Lower power consumption
- ❑ Reduced noise, sophisticated speed control

(a)

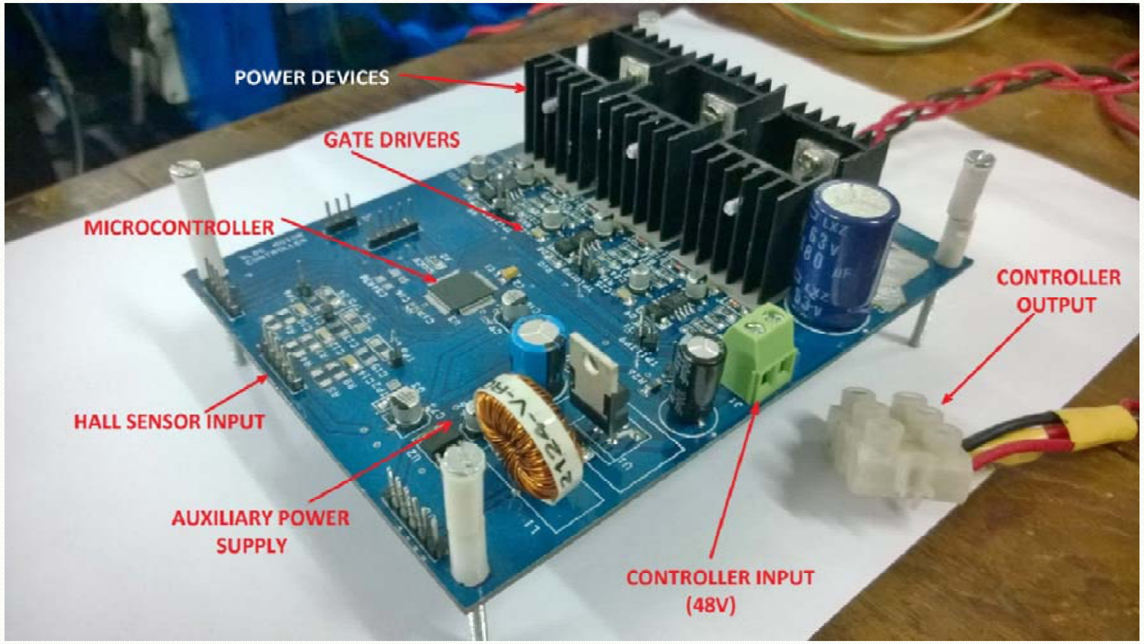

(b)

Fig. (a) The DC mixer grinder retrofitted with the BLDC motor and (b) its controller[1].

---

[1] C. D. Bhagat, S. P. Nikam and B. G. Fernandes, "Design and development of sensorless controller for DC-operated mixer-grinder," SGBC *2016*, 2016, pp. 1-6, doi: 10.1109/SGBC.2016.7936065.

Permanent Magnet DC Motor Directly Powered by Solar PV Panel

- Coarse MPPT operation is performed without using a power electronic converter.

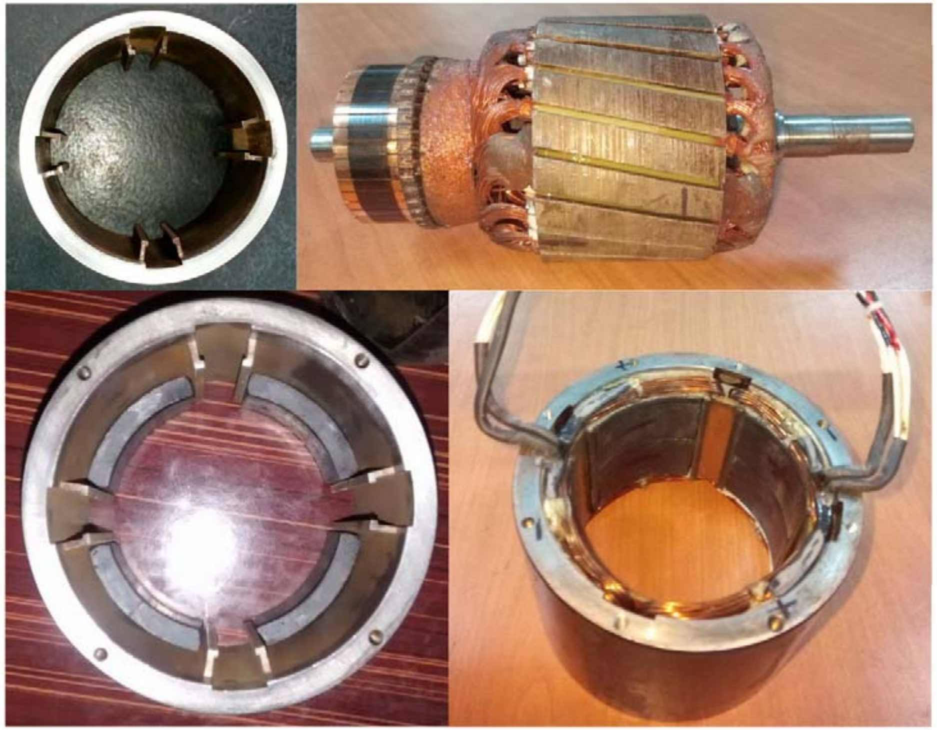

(a)

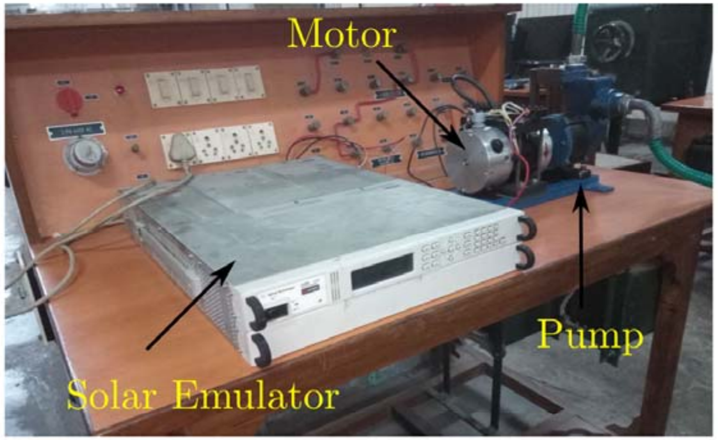

(b)

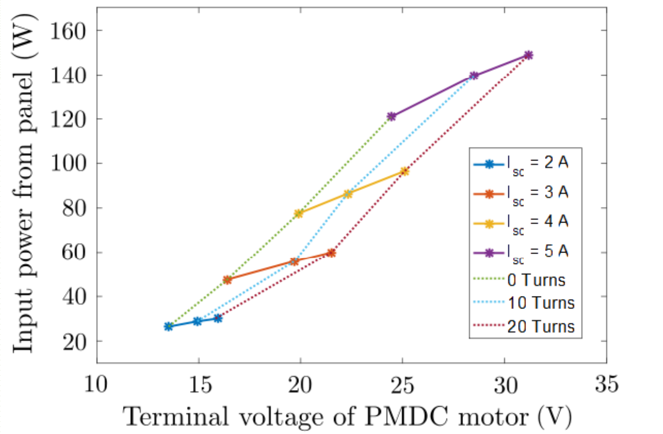

(c)

Fig. (a) Stator, rotor and yoke of the experimental prototype before the final assembly, (b) The experimental setup and (c) the measured voltage vs. power (V-P) characteristics.

An OVERVIEW of Research and Development Activities in **GaN based PE Converter,** Integration of RES, DC Microgrid, High-power Converter, and SST

PEPS, EE Department,

IIT Bombay

GaN Based Interleaved Isolated Boost Converter

- Interleaved boost converter to boost 48 V to 400 V.
- Planar magnetics is used to reduce the height and obtain low profile of converter assembly.

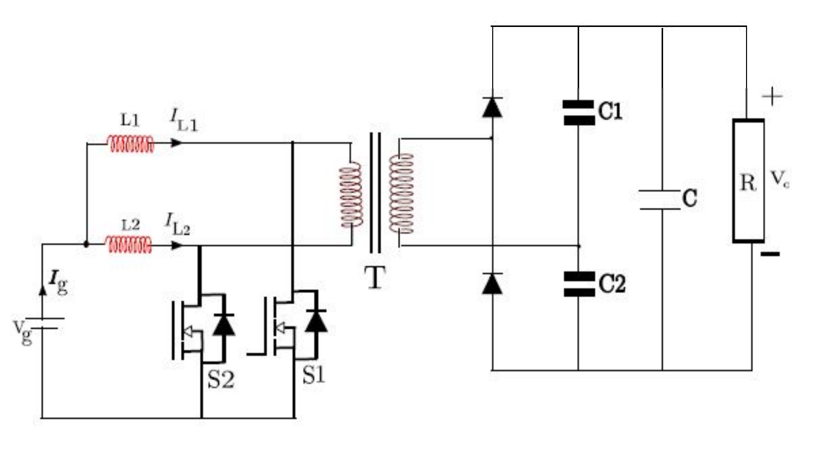

(a)

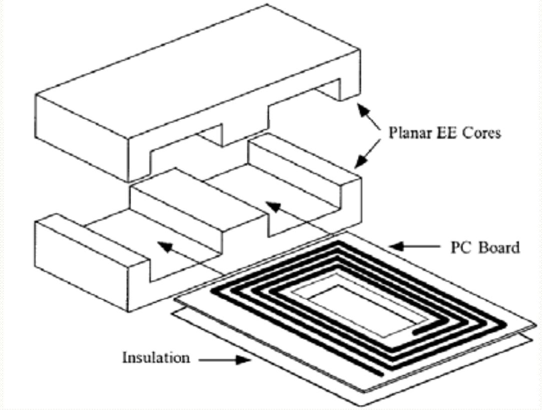

(b)

(c)

Fig. (a) Schematic of proposed interleaved isolated boost converter[1] , (b) Planar transformer core and PCB winding, and (c) PCB of the fabricated converter.

---

[1] S. Akshatha, R. Vinayak and B. G. Fernandes, "Isolated Dual Boost Converter: Controller Design using Affine Parameterisation," PEDES 2018, pp. 1-6, doi: 10.1109/PEDES.2018.8707597.

GaN Based Half-bridge DC-DC converter for Ultracapacitor Interface

- ❑ Switching frequency is 1MHz.
- ❑ Power Circuit, controller and sensing are incorporated on a single PCB.

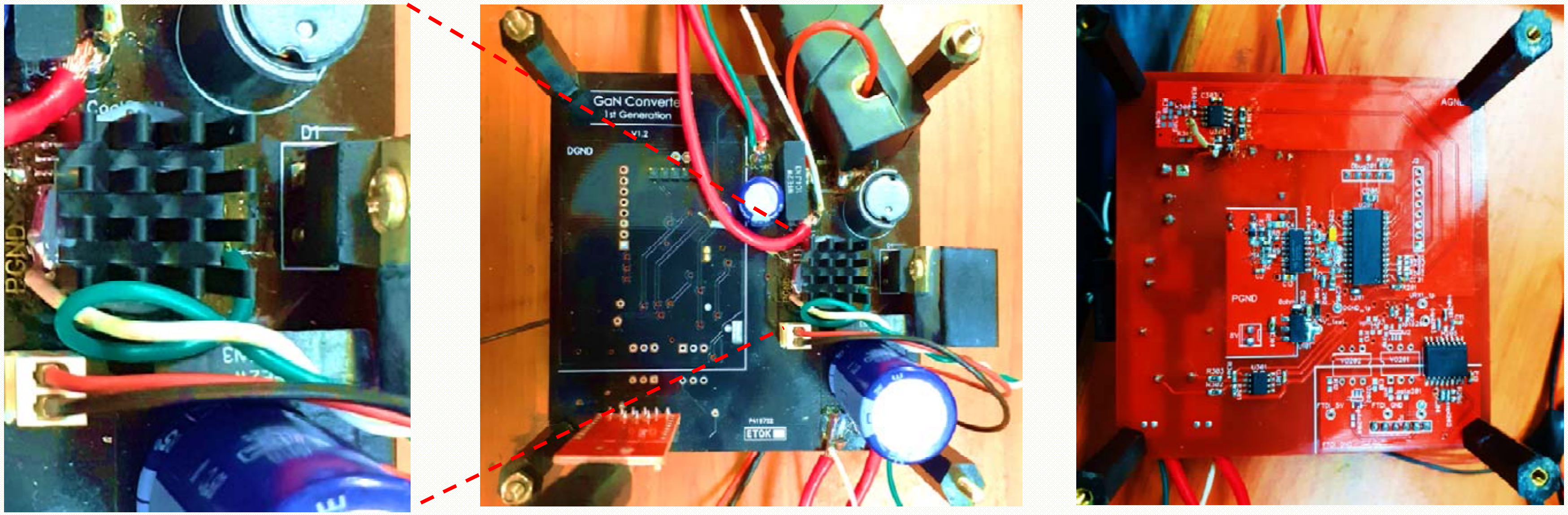

(a) (b) (c)

Fig. (a) Zoomed view of the GaN device (Infineon CoolGaN series GaN HEMT) along with its heatsink, (b) Top and (c) Bottom views of the fabricated PCB.

GaN Based Half Bridge Leg Designed for 1 kW Totem pole PFC

- 4 layer PCB is adapted; TI's integrated GaN IC has been used to further reduce the parasitic inductance.
- Power Circuit, controller and sensing are incorporated on a single PCB.
- Converter ratings: Input voltage (rms) (115 v – 230 V), Ouput voltage (390 V), Output power (1 kW), Switching frequency (100 kHz).

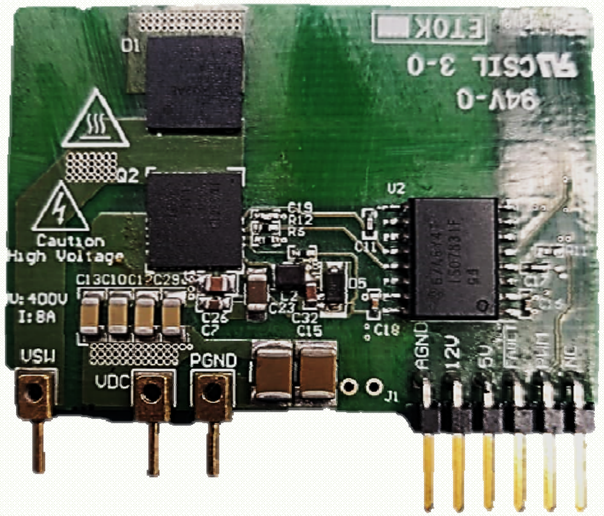

(a) (b)

Fig. (a) GaN device (TI GaN HEMT: 600 V, 12 A, Rdson = 12 mΩ) based half bridge leg and (b) the fabricated converter assembly for 1 kW bridgeless PFC.

An OVERVIEW of Research and Development Activities in GaN based PE Converter, Integration of RES, DC Microgrid, High-power Converter, and SST

Prof. Baylon G. Fernandes

Department of Electrical Engineering,

Indian Institute of Technology Bombay

- A novel active power decoupling topology is proposed with fault tolerant ability, which
  - eliminates the need of bulk electrolytic capacitors by implementing active power decoupling with the help of an auxiliary circuit,
  - can deliver 50% of the rated power along with ripple power compensation under fault tolerant operation.

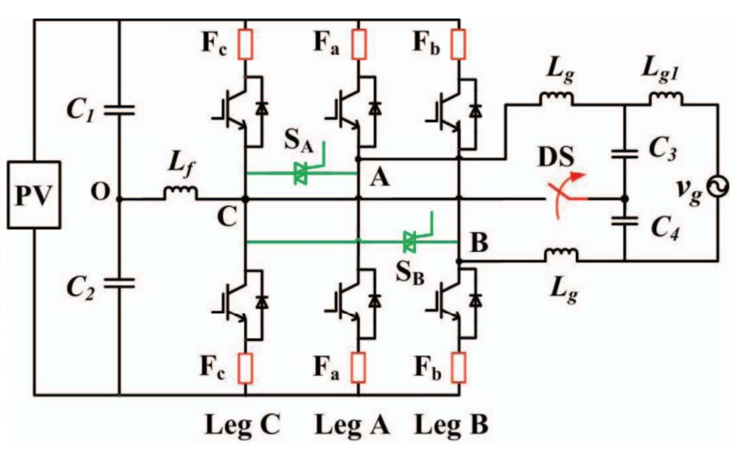

(a)

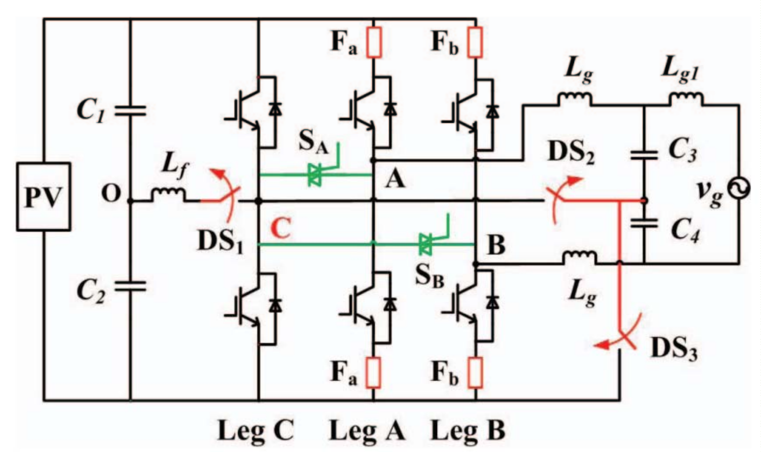

(b)

Fig. The proposed converter reconfiguration with the ripple power compensation on (a) the DC side and (b) the AC side[1].

---

[1] V. V. S. Pradeep Kumar and B. G. Fernandes, "Active power decoupling topology with fault tolerant ability for a single phase grid connected inverter," *IECON 2015 - 41st Annual Conference of the IEEE Industrial Electronics Society*, 2015, pp. 003423-003428, doi: 10.1109/IECON.2015.7392629.

A Fault-Tolerant Single-Phase Grid-Connected Inverter Topology With Enhanced Reliability for Solar PV Applications

- A single-phase fault-tolerant inverter topology is proposed, which
  - does not use the redundant leg, and
  - achieves the fault-tolerant feature with minimal device count.
- Moreover, the reliability of the proposed topology is calculated to be more than that of the redundant leg-based topologies.

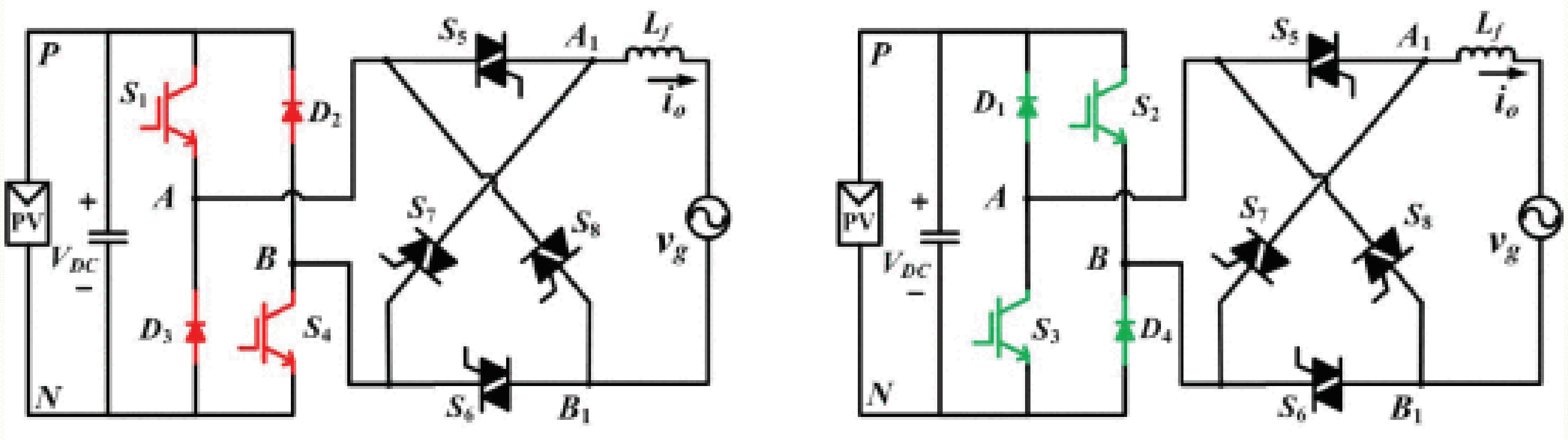

(a) (b)

Fig. Redundancy in the proposed topology[1].

---

[1] V. V. S. Pradeep Kumar and B. G. Fernandes, "A Fault-Tolerant Single-Phase Grid-Connected Inverter Topology With Enhanced Reliability for Solar PV Applications," in *IEEE Journal of Emerging and Selected Topics in Power Electronics*, vol. 5, no. 3, pp. 1254-1262, Sept. 2017, doi: 10.1109/JESTPE.2017.2687126.

A Low Cost Reliable Stand-Alone Photovoltaic System

- A 250 VA battery integrated stand-alone PV system is proposed, which
  - has higher life time than other conventional PV systems,
  - implement on low cost micro-controller with fewer sensing components.,
  - can be designed for a 12 V or 24 V PV panels (commonly used in rural areas).

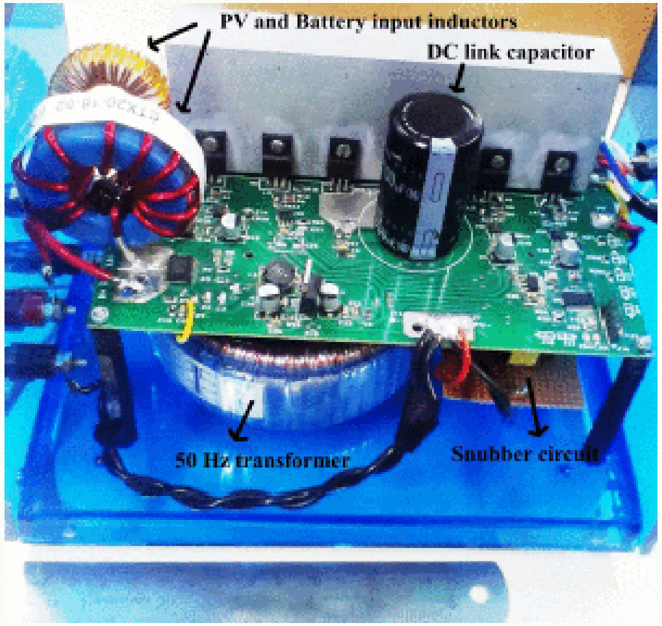

Fig. The 250 VA laboratory scale prototype is shown[1].

[1] R. S. Farswan, H. Khan and B. G. Fernandes, "A low cost reliable stand-alone photo-voltaic system," *2014 IEEE International Conference on Power Electronics, Drives and Energy Systems (PEDES)*, 2014, pp. 1-6, doi: 10.1109/PEDES.2014.7042143.

Development of a Two-Stage Transformerless Grid-Tied PV Inverter System Using SiC Devices

- ❑ A two-stage transformerless single-phase grid-tied PV system is developed for residential rooftop application.
  - ❑ It has a very low leakage current → no galvanic isolation required at any stage.
  - ❑ SiC based devices → high system efficiency, reduced size of magnetics.

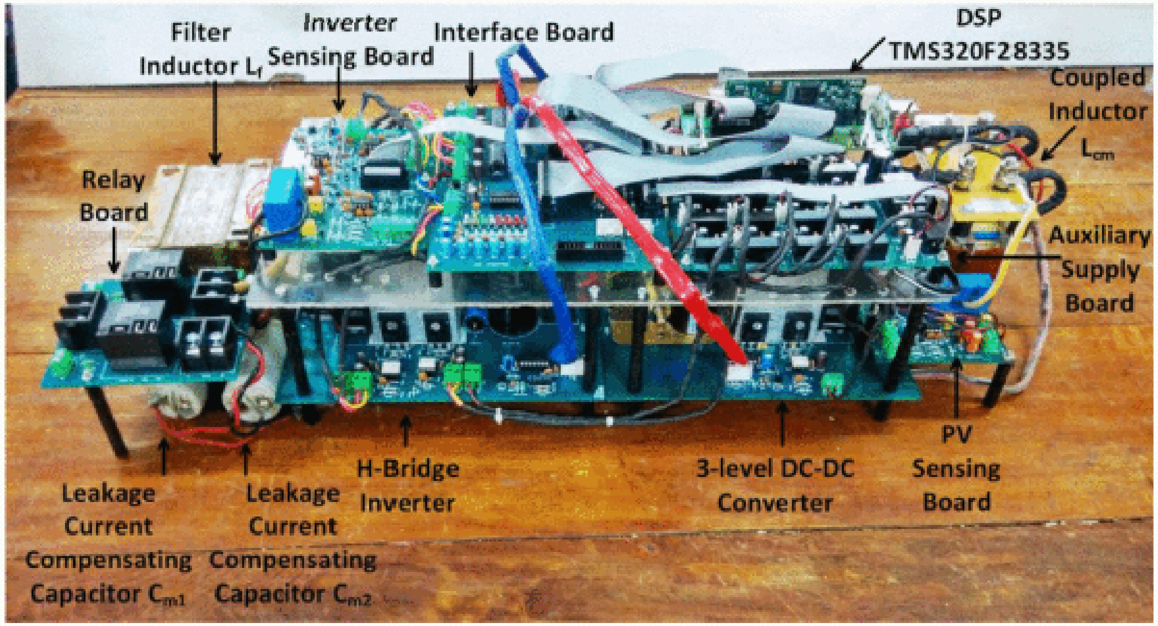

Fig. The 2.5 kVA laboratory scale prototype is shown[1].

---

[1] A. Datta, R. S. Farswan and B. G. Fernandes, "Development of a two-stage transformerless grid-tied photovoltaic inverter system using SiC devices," *2017 IEEE Applied Power Electronics Conference and Exposition (APEC)*, 2017, pp. 2964-2969, doi: 10.1109/APEC.2017.7931118.

Reliable and Effective Ride-Through Controller Operation for Smart PV Systems Connected to Low Voltage Distribution Grid

- A smart low-voltage (LV) ride-through (RT) controller for PVs connected at high penetration to LV grid is proposed to perform ancillary features, such as voltage support (VS), ride-through (RT) operation, and islanding detection.

(a)

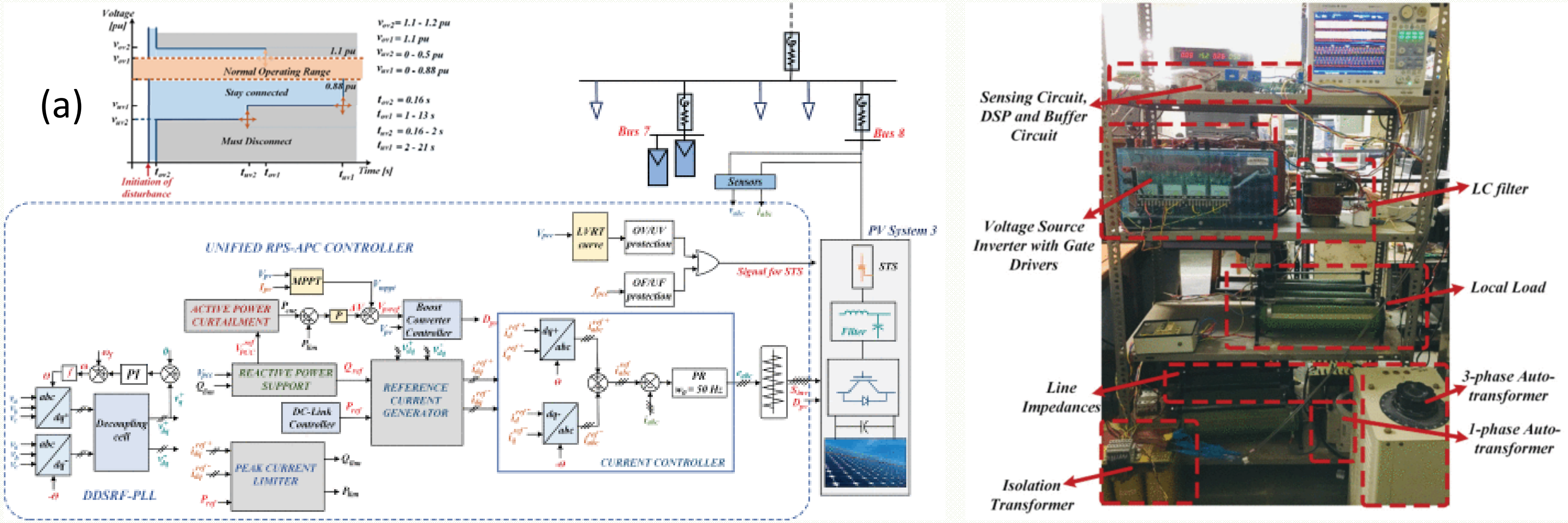

(b) (c)

Fig. (a) Extended clearing time in response to abnormal grid voltages as defined in amendment IEEE 1547a , (b) Unified RPS-APC controller, and (c) Experimental setup[1].

---

[1] H. Khan, S. J. Chacko, B. G. Fernandes and A. Kulkarni, "Reliable and Effective Ride-Through Controller Operation for Smart PV Systems Connected to LV Distribution Grid Under Abnormal Voltages," in *IEEE Journal of Emerging and Selected Topics in Power Electronics*, vol. 8, no. 3, pp. 2371-2384, Sept. 2020, doi: 10.1109/JESTPE.2019.2918620.

Integration of Low-voltage PV With AC Grid Employing a Unified AC-DC System

- Integration of a renewable energy source (RES) with ac grid is examined using a three-phase PWM rectifier and low voltage (LV) photovoltaic (PV).[1,2]
- It introduces multifunctionality using a single PWM converter.

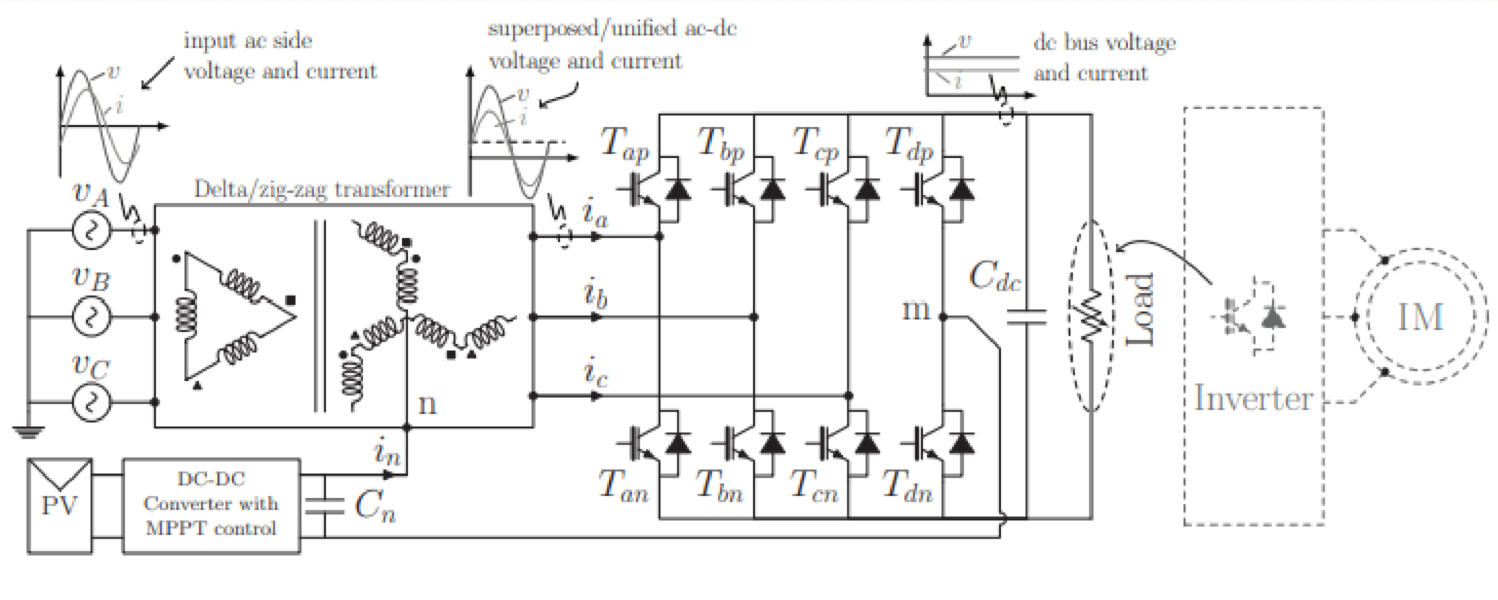

Fig. The proposed scheme uses a line-frequency zig-zag transformer and a single three-phase four-leg PWM rectifier to integrate the low voltage PV with three-phase ac grid.

[1] A. Shetty, B. G. Fernandes, O. Ojo, and J. A. Ferreira, “Low-voltage pv power integration for variable frequency drives application,” in EPE 2017, Sept 2017, pp. P.1–P.10.

[2] V. Chitransh, A. Shetty, A. K. Das, J. O. Ojo, M. Veerachary, B. G. Feranandes and J. A. Ferreira, "Evaluation of Multifrequency Power Electronic Converters: Concept, Architectures, and Realization," in *IEEE Journal of Emerging and Selected Topics in Power Electronics*, vol. 9, no. 3, pp. 3582-3597, June 2021, doi: 10.1109/JESTPE.2020.3019730.

Design Methodology of a Line-frequency Zig-Zag Transformer in a Unified AC-DC System

- Overall power density of the UACDC converter system is improved as the additional boost reactors are omitted by utilizing the leakage inductance of transformer.[1]
- Aiding effect of interleaved winding strategy is studied which helps integrating the low voltage PV with the ac grid[2].

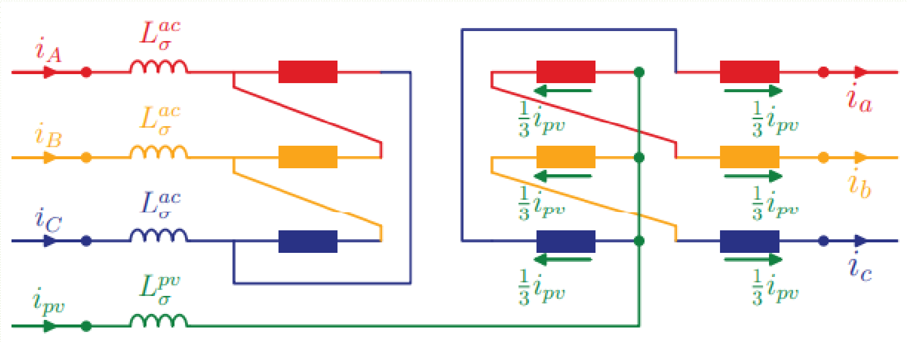

(a)

(b)

Fig. Proposed scheme depicts the integration of low voltage (LV) photovoltaic (PV) with ac grid using a single three-phase four-leg PWM rectifier.

[1] A. K. Das, A. Shetty and B. G. Fernandes, "Design Methodology of a Line-Frequency Zig-Zag Transformer to Utilize its Winding Leakage Inductances as Integrated Boost-Inductances in a Unified AC-DC System," ECCE 2018, pp. 3198-3205, doi: 10.1109/ECCE.2018.8557912.
[2] A. K. Das, A. Shetty and B. G. Fernandes, "Aiding Effects of Interleaving to Improve Design Performances of a Line-frequency Zig-Zag Transformer Employed in a Unified AC-DC System," PEDES 2020, pp. 1-6, doi: 10.1109/PEDES49360.2020.9379875.

- A novel topology of integrating the battery without the need of a seperate converter for the automotive generator is proposed, which reduces size and weight.[1]

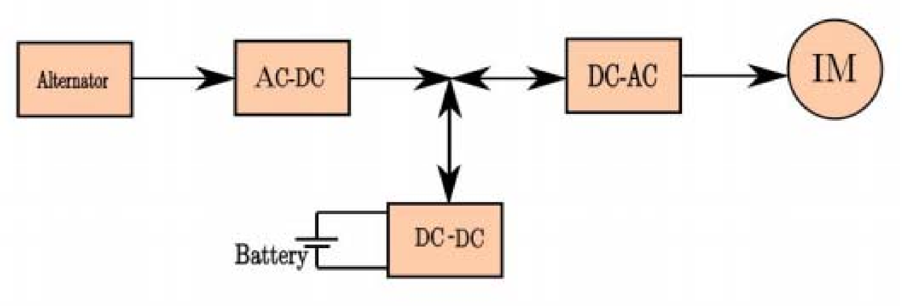

(a)

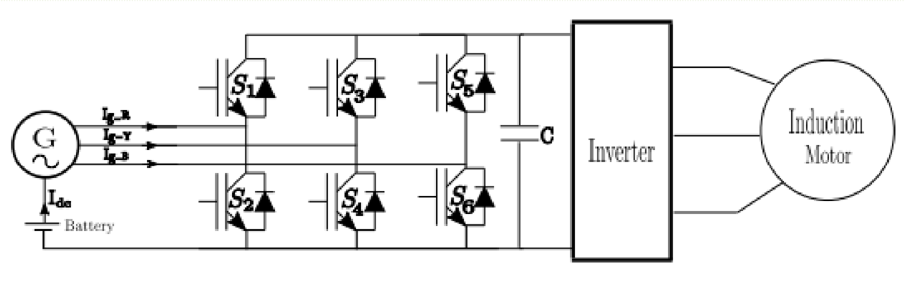

(b)

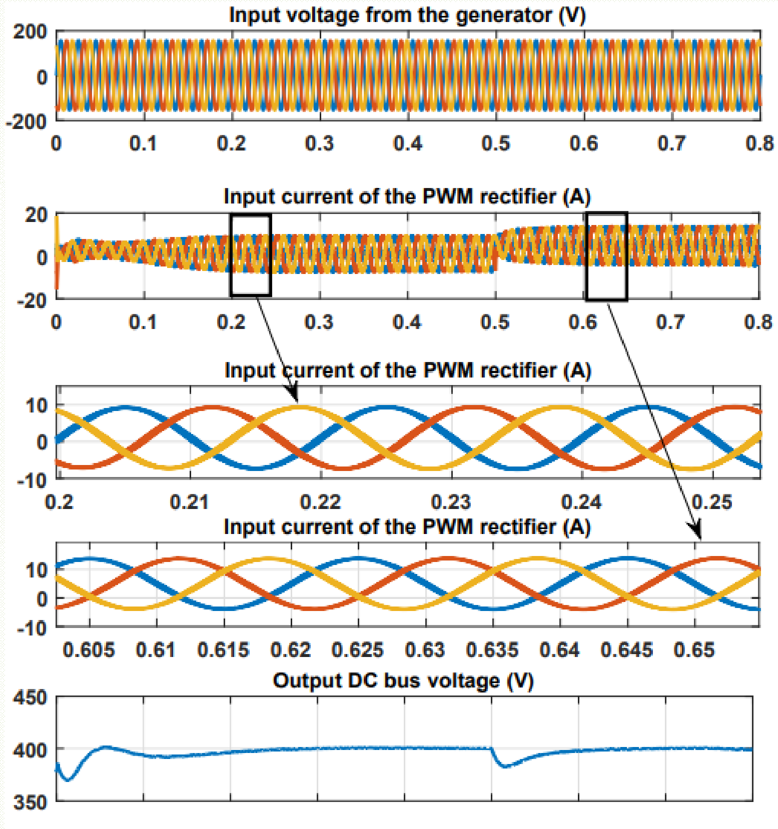

Fig. (a) Power train arrangement for a series HEV, (b) the proposed PWM rectifier topology, and (c) Performance during battery in discharging mode[1].

(c)

[1] A. Shetty, B. G. Fernandes, J. O. Ojo and J. A. Ferreira, "Three Phase PWM Rectifier with Integrated Battery for Automotive Applications," IAS 2018, pp. 1-6, doi: 10.1109/IAS.2018.8544681.

An OVERVIEW of Research and Development Activities in GaN based PE Converter, Integration of RES, DC Microgrid, High-power Converter, and SST

Prof. Baylon G. Fernandes

Department of Electrical Engineering,

Indian Institute of Technology Bombay

Optimal Voltage Level for DC Microgrids

- The proposed dc systems offer 15–22% and 10–11% improvement over the conventional ac system in operating efficiency for residential and commercial systems respectively.[1]
  - For residential dc system, low voltage system (48V) is an optimal choice, whereas
  - For commercial facilities, medium voltage level (400V) offers the highest operating efficiency.

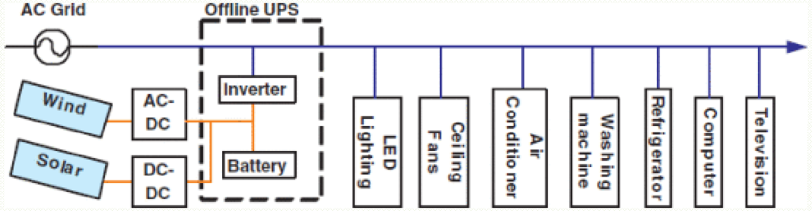

(a)

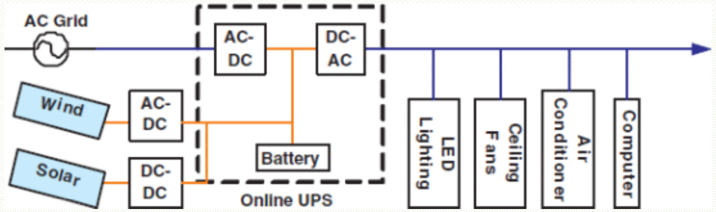

(b)

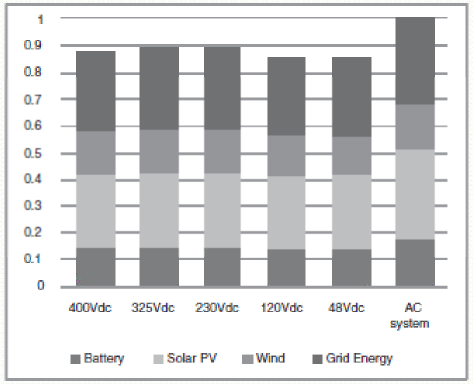

(c)

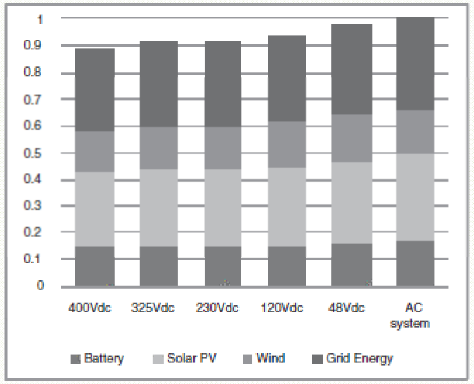

(d)

Fig. (a) AC residential and (b) AC commercial systems, and Comparison of dc and ac systems for (c) residential and (d) commercial applications[1].

[1] S. Anand and B. G. Fernandes, "Optimal voltage level for DC microgrids," *IECON 2010 - 36th Annual Conference on IEEE Industrial Electronics Society*, 2010, pp. 3034-3039, doi: 10.1109/IECON.2010.5674947.

Bidirectional Z-Source Breaker for DC Micro-grid Protection

- Fast operating bidirectional solid state circuit breakers are developed which are suitable for protection of dc systems.[1],[2]

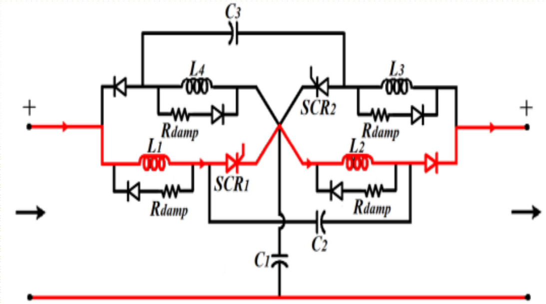

(a)

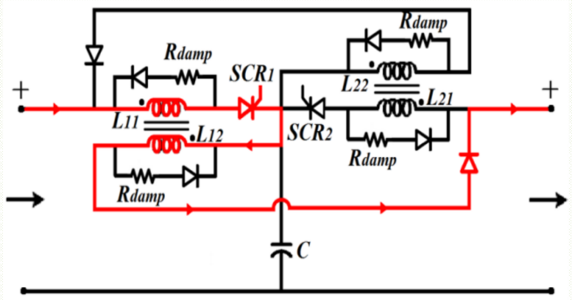

(b)

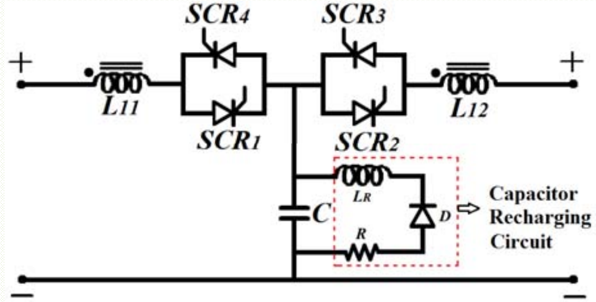

(c)

Fig. (a-c) Proposed topologies of the bidirectional Z-source breakers (Bi-ZSB)[1,2], and (d-e) the fabricated laboratory scale prototypes.

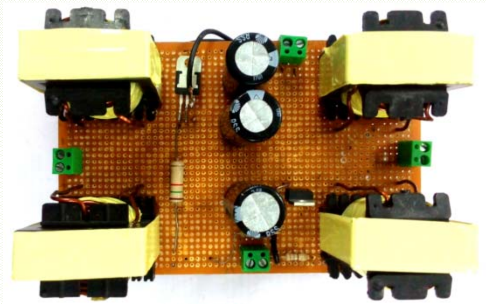

(d)

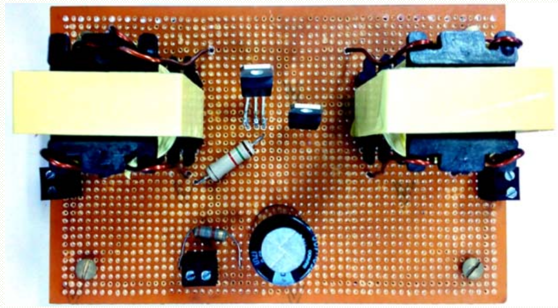

(e)

[1] S. G. Savaliya and B. G. Fernandes, "Analysis and Experimental Validation of Bidirectional Z-Source DC Circuit Breakers," in *IEEE Transactions on Industrial Electronics*, vol. 67, no. 6, pp. 4613-4622, June 2020.
[2] S. G. Savaliya and B. G. Fernandes, "Performance Evaluation of a Modified Bidirectional Z-Source Breaker," in *IEEE Transactions on Industrial Electronics*, vol. 68, no. 8, pp. 7137-7145, Aug. 2021.

❑ Cell balancing, Accurate estimation of the State of Charge (SOC), and Online estimation of the State of Health (SoH).[1]

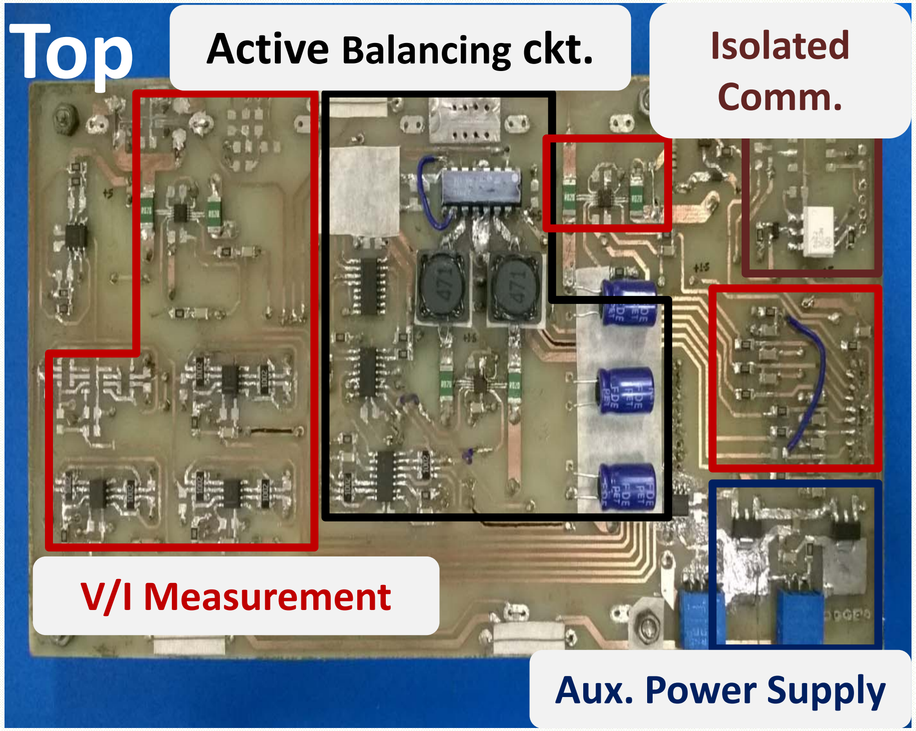

(a)

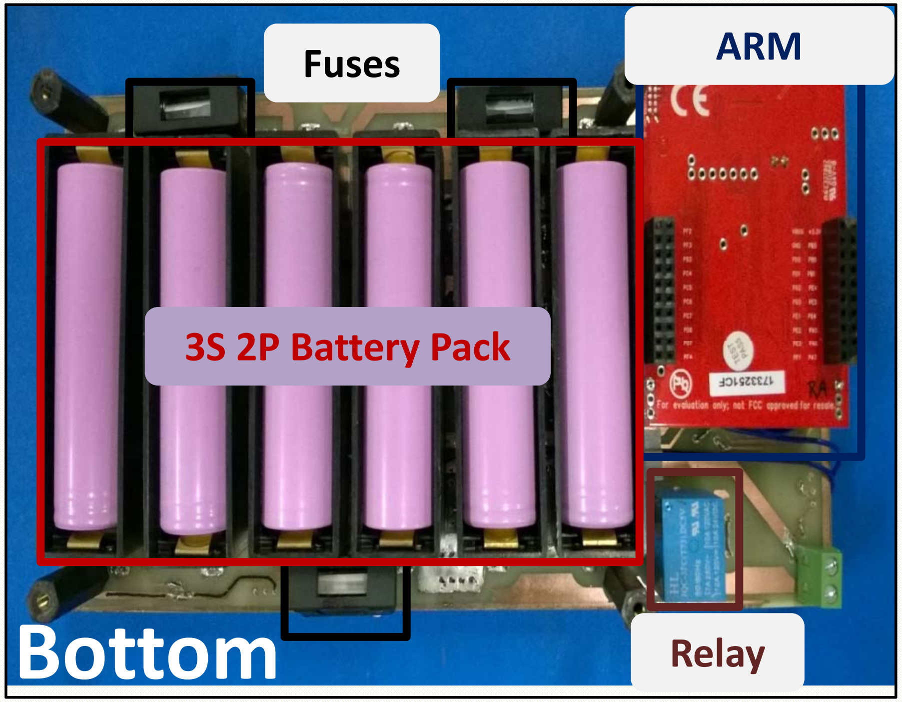

(b)

Fig. (a) Top and (b) Bottom views of the fabricated battery management system[1].

[1] R. Anand and B. G. Fernandes, "Simplified control strategy for an inhomogeneous series-connected battery string," ECCE 2019, pp. 5064-5071, doi: 10.1109/ECCE.2019.8913308.

An OVERVIEW of Research and Development Activities in GaN based PE Converter, Integration of RES, DC Microgrid, High-power Converter, and SST

Prof. Baylon G. Fernandes

Department of Electrical Engineering,

Indian Institute of Technology Bombay

A 9-level Hybrid Symmetric Cascaded Multilevel Converter for Induction Motor Drive

- ❑The proposed converter is capable of producing nine output voltage levels by using the same number of power cells as that of a conventional five-level symmetric cascaded H-bridge converter.[1]

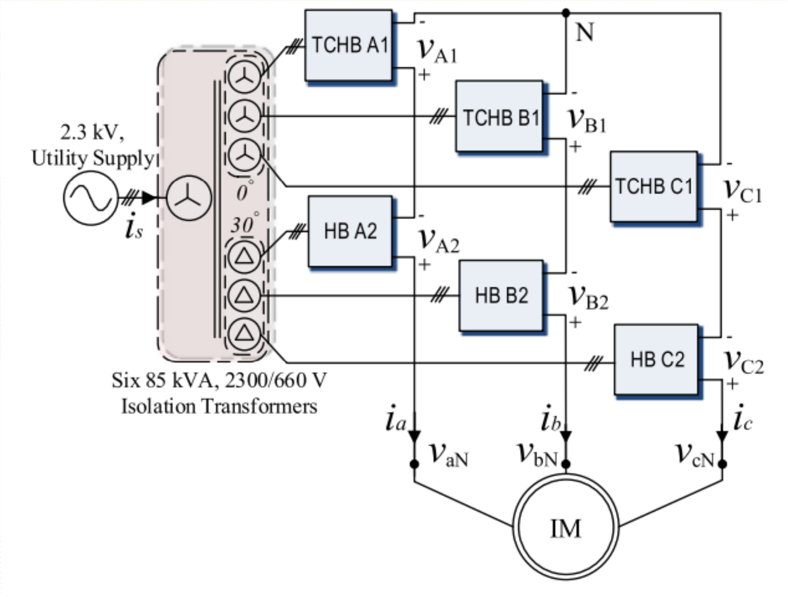

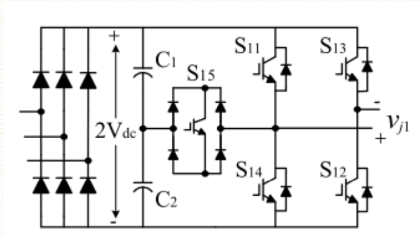

(b)

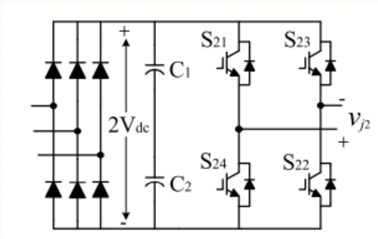

(a) (c) (d)

Fig. (a) System architecture, (b-c) TCHB and HB power cells, and (b) Experimental setup[1].

---

[1] Indrajit Sarkar and B. G. Fernandes, "A nine-level hybrid symmetric cascaded multilevel converter for induction motor drive", Sadhana, vol. 42, no. 8, pp. 1389-1400, Aug 2017.

Modular Transformer-based Regenerative CMC Converter for drives with Multilevel operation at Input & Output

- A configuration of cascaded multicell converter (CMC) with single phase PWM rectifier-power cell is proposed in [1] for MV high-power regenerative drives.[1]

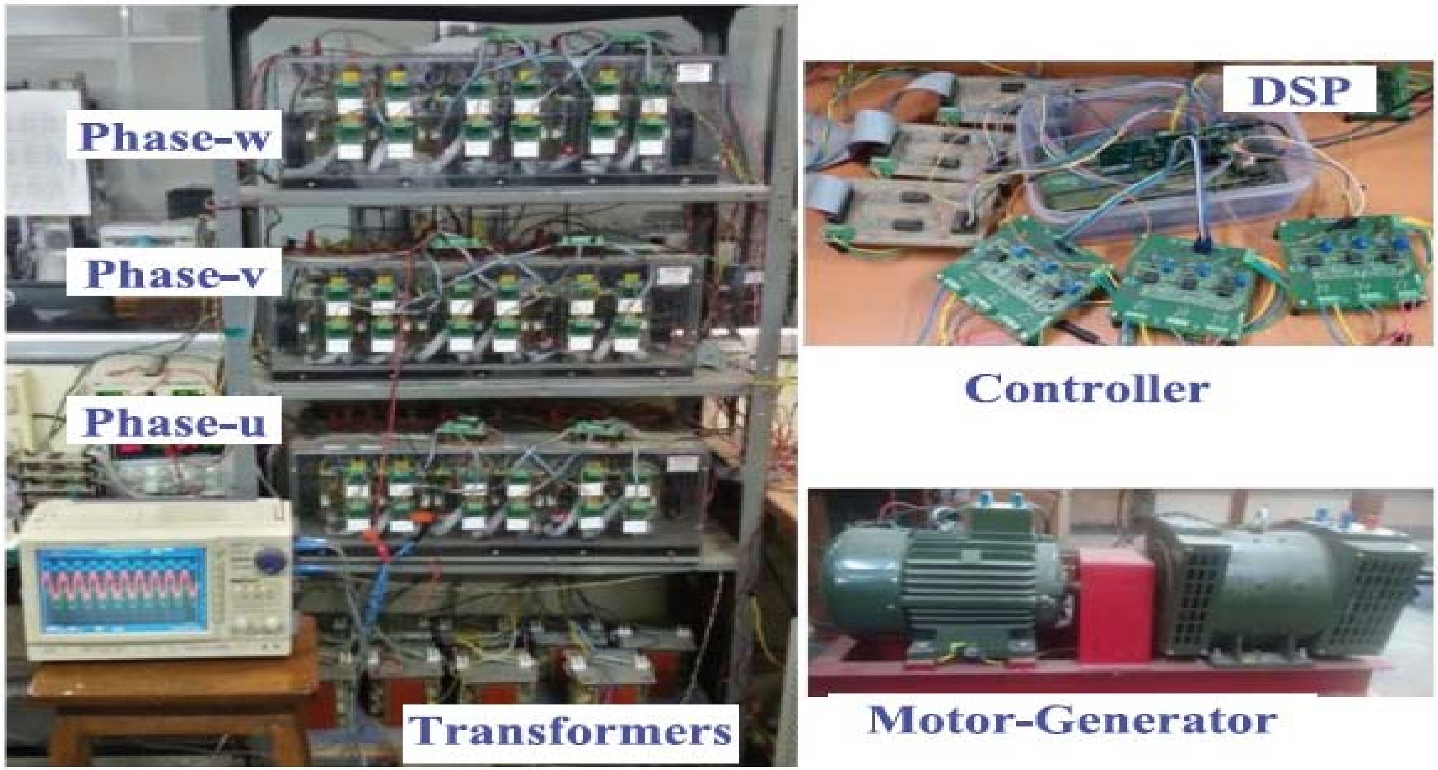

Fig. Experimental setup showing converter modules, DSP and motor-generator load[1].

[1] S. Sau, S. Karmakar and B. G. Fernandes, "Modular Transformer-Based Regenerative-Cascaded Multicell Converter for Drives With Multilevel Voltage Operation at Both Input and Output Sides," in *IEEE Transactions on Industrial Electronics*, vol. 65, no. 7, pp. 5313-5323, July 2018, doi: 10.1109/TIE.2017.2774733.

Modular Multilevel Converter Based Variable Speed Drive with Reduced Capacitor Ripple Voltage

- ❑ A new configuration of multi-pulse diode-bridge rectifier circuit is proposed.[1]
- ❑ It reduces the dc-bus voltage as speed reduces, is cost-effective, simple and robust solution for non-regenerative variable speed drive (VSD) application.

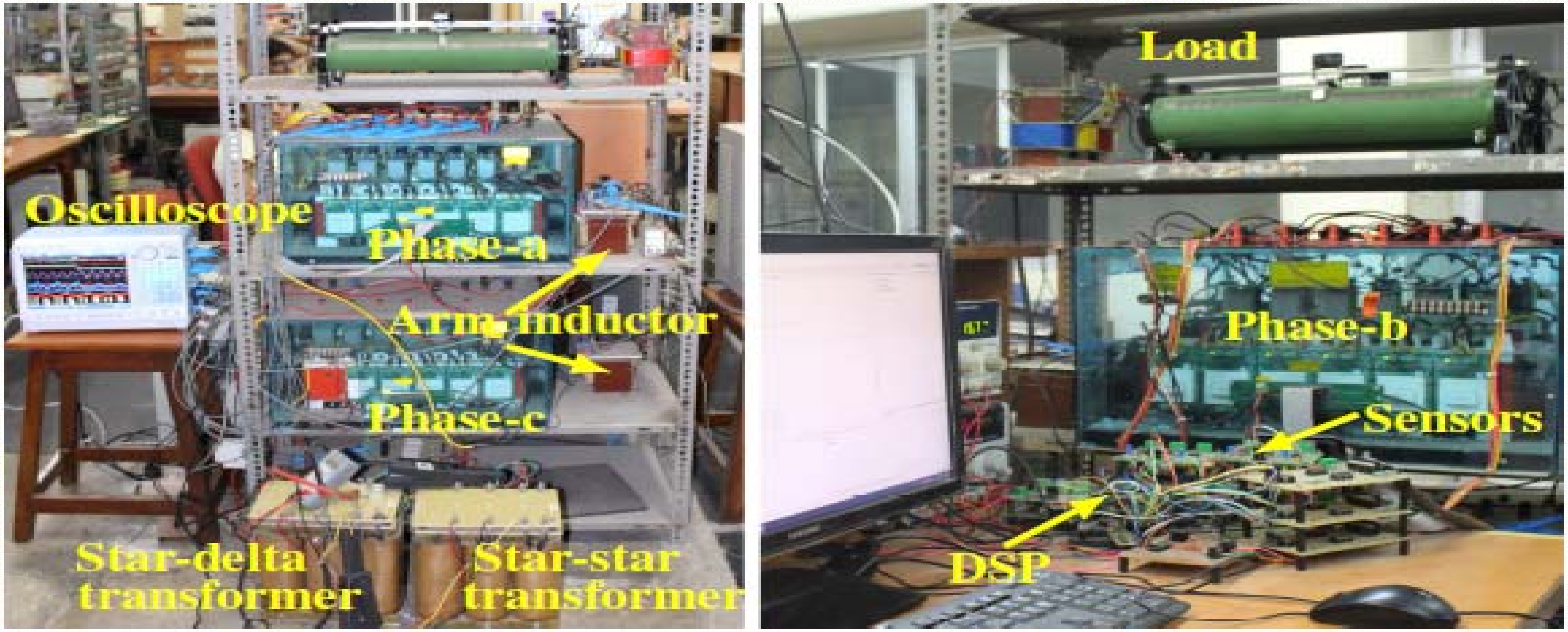

Fig. Experimental setup showing converter modules, DSP and motor-generator load[1].

[1] S. Sau and B. G. Fernandes, "Modular Multilevel Converter Based Variable Speed Drive With Reduced Capacitor Ripple Voltage," in *IEEE Transactions on Industrial Electronics*, vol. 66, no. 5, pp. 3412-3421, May 2019, doi: 10.1109/TIE.2018.2860542.

Elimination of Power Unbalance in Phases of CHB Converter for PV Integration

- Power unbalance in phases of CHB under unequal PV power generation is eliminated.[1]
- The DC-DC converter, connecting PV modules to the CHB, contains a high-frequency transformer with single input and three outputs; it tracks the MPP, provides isolation and eliminates the power unbalance in the phases of CHB.

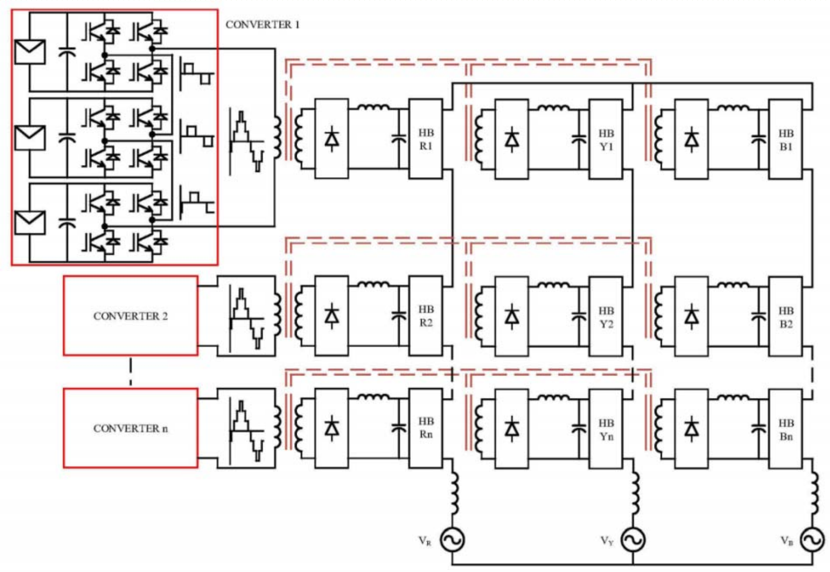

(a)

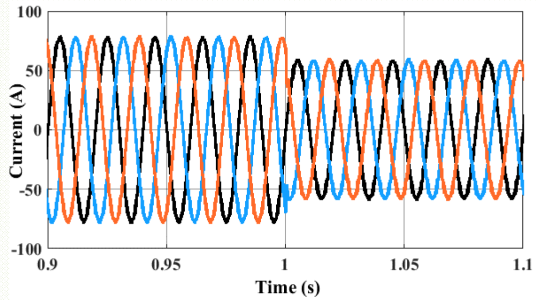

(b)

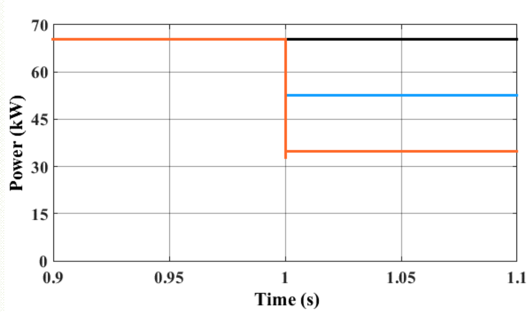

(c)

Fig. (a) Proposed converter, and Simulation results showing (b) Grid current and (c) PV generation[1].

---

[1] K. A. Ajith and B. G. Fernandes, "Elimination of Phase Unbalance in Cascaded Multilevel Converters for Large-Scale Photovoltaic Grid Integration," IAS 2019, pp. 1-5, doi: 10.1109/IAS.2019.8912358.

A Multiport Converter Interfacing Solar PV Modules and Energy Storage With DC Microgrid

- A novel multiport converter (MPC) is proposed to interface different solar photovoltaic modules (SPM), and the battery with a 380 V dc microgrid.[1]
  - In the microgrid-connected mode, it is capable of realizing the MPP tracking and controlling the battery charging current as per the SOC controller.
  - In the stand-alone mode, the voltage across the local loads are regulated at 380 V.

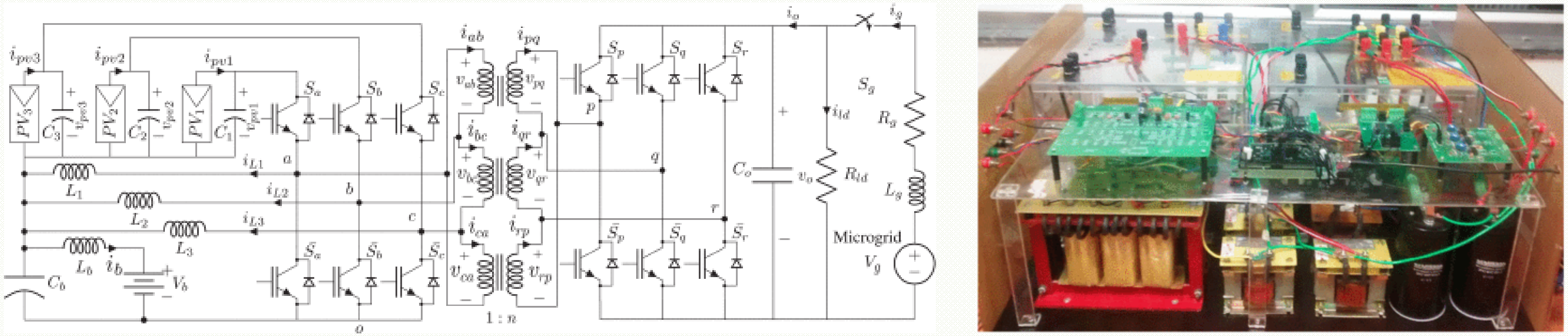

(a) (b)

Fig. (a) Schematic circuit diagram of the proposed MPC, and (b) Photograph of the developed laboratory prototype[1].

---

[1] A. Vettuparambil, K. Chatterjee and B. G. Fernandes, "A Multiport Converter Interfacing Solar Photovoltaic Modules and Energy Storage With DC Microgrid," in *IEEE Transactions on Industrial Electronics*, vol. 68, no. 4, pp. 3113-3123, April 2021, doi: 10.1109/TIE.2020.2978709.

An OVERVIEW of Research and Development Activities in GaN based PE Converter, Integration of RES, DC Microgrid, High-power Converter, and SST

Prof. Baylon G. Fernandes

Department of Electrical Engineering,

Indian Institute of Technology Bombay

A SST based Fast Charging Station for All Categories of Electric Vehicles

- Using SST topology, it integrates renewable energy sources (RES)such as PV and battery to each fast charging (FC) port.[1]
- It conforms to Level 3 dc fast charging of three different classes of electric vehicles (EV).

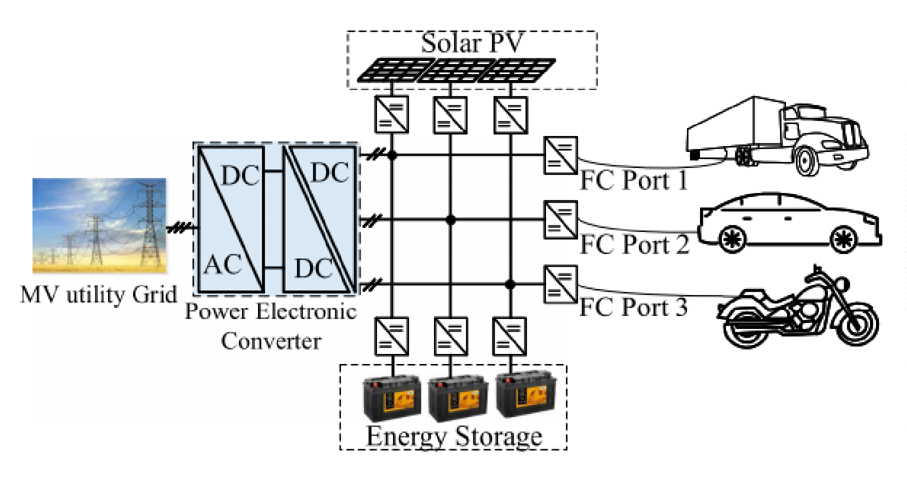

(a)

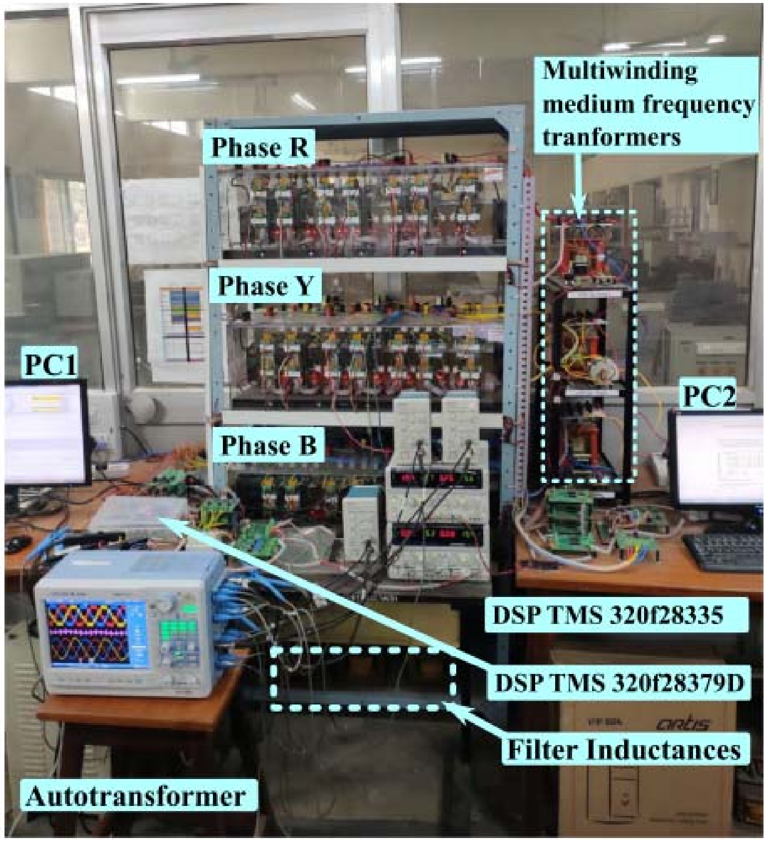

(b)

Fig. (a) Structure of the fast charging station, and (b) Laboratory scale hardware setup[1].

---

[1] A. C. Nair and B. G. Fernandes, "Solid-State Transformer Based Fast Charging Station for Various Categories of Electric Vehicles With Batteries of Vastly Different Ratings," in *IEEE Transactions on Industrial Electronics*, vol. 68, no. 11, pp. 10400-10411, Nov. 2021, doi: 10.1109/TIE.2020.3038091.

A Quad Active Bridge (QAB) based On-board Power Electronic Interface for an Electric Vehicle

- ❑A QAB converter is proposed which acts as an on-board power electronic interface for an electric vehicle.[1]
- ❑Power management scheme for the operation of the electric vehicle with QAB interface.
- ❑Control strategy for effective power sharing between battery and ultra-capacitor (UC).
- ❑Simulation studies and Experimental results to verify the effectiveness of the HESS control in sharing the power between UC and battery.

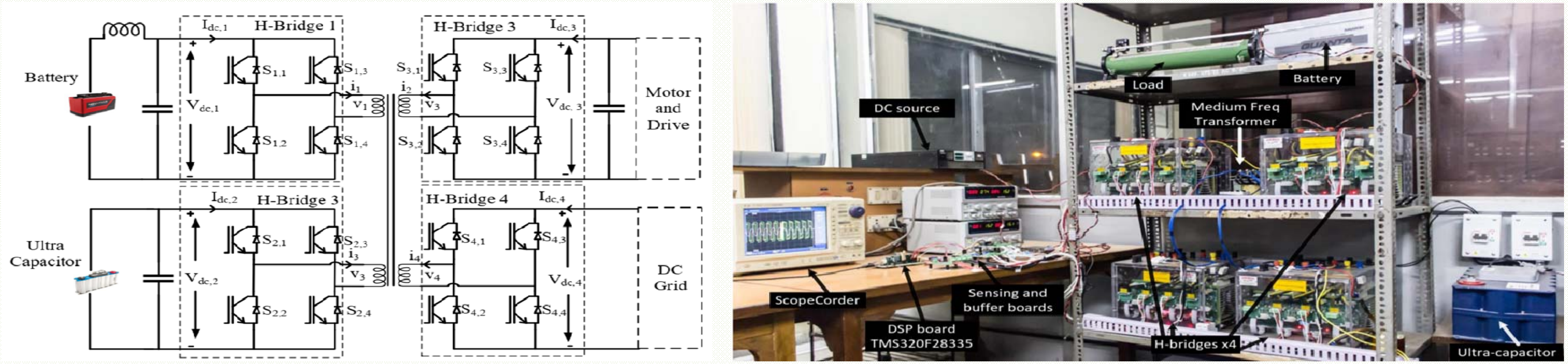

(a) (b)

Fig. (a) Proposed QAB converter allows power transfer from HESS to drive and charging from a DC grid, and (b) Laboratory scale hardware setup[1].

---

[1] A. C. Nair, Vishal M.J. and B.G. Fernandes "A Quad Active Bridge based On-board Power Electronic Interface for an Electric Vehicle," *2018 IEEE Energy Conversion Congress and Exposition (ECCE)*, Portland, Oregon, 2018.

Minimum RMS Current Operation of Isolated DAB DC-DC Converter Employing DPS Control

- Universal trajectory is derived for dual phase-shift (DPS) control of a DAB converter to minimize the reactive power flow and thereby improve the efficiency.[1]

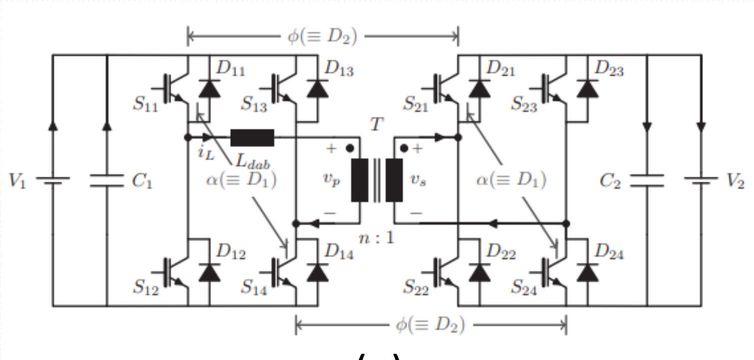

(a)

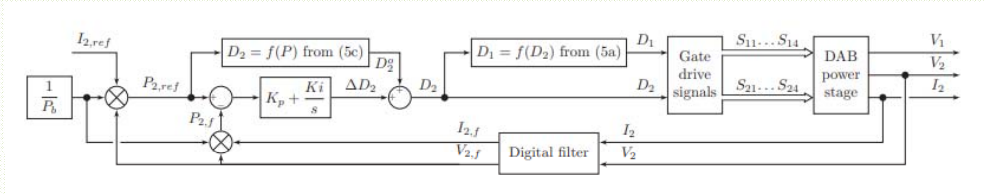

(d)

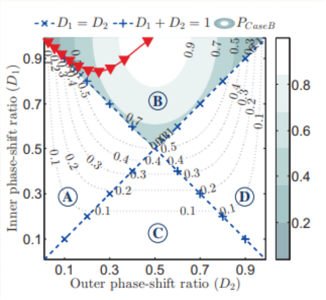

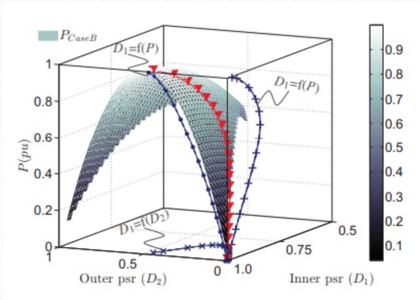

(b) (c)

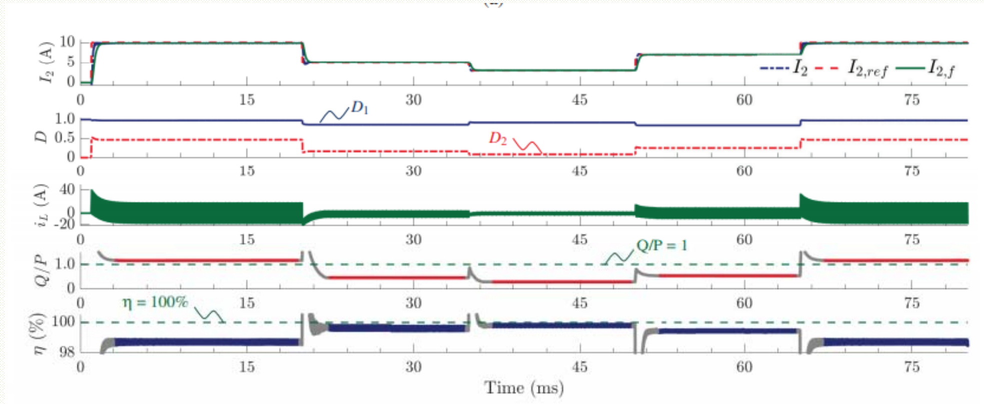

(e)

Fig. (a) Schematic of a DAB converter, (b-c) The proposed minimum rms current trajectory, and (d-e) The closed-loop control and simulation results[1].

[1] A. K. Das and B. G. Fernandes, "Fully ZVS, Minimum RMS Current Operation of Isolated Dual Active Bridge DC-DC Converter Employing Dual Phase-Shift Control," EPE 2019, pp. P.1-P.10, doi: 10.23919/EPE.2019.8914975.

❑ Natural resonance frequencies of a high-frequency two-winding transformer are estimated analytically using an equivalent pi-model representation.[1]

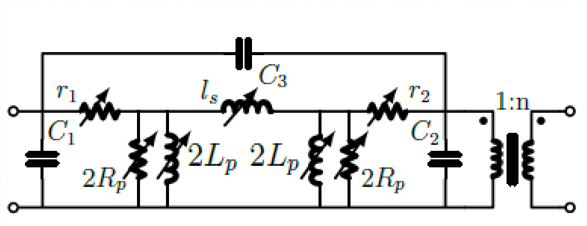

(a)

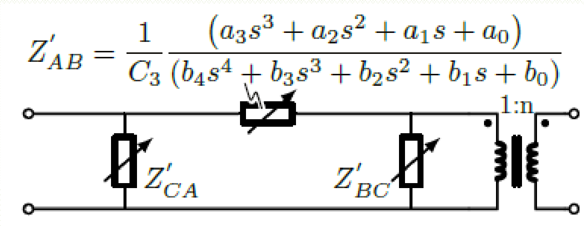

(b)

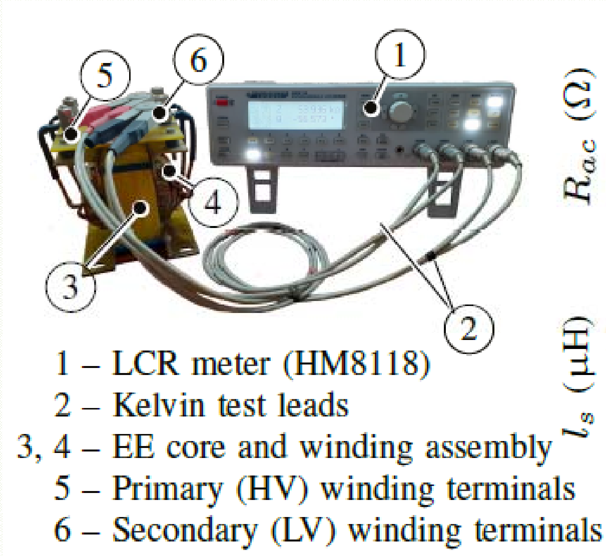

(c)

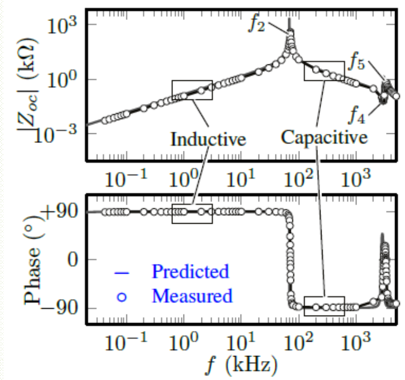

(d)

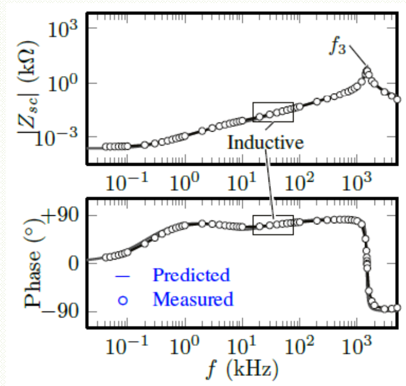

(e)

Fig. (a) Capacitive pi-model of a high-frequency two-winding transformer and (b) its equivalent transfer function based representation, (c) Lumped circuit measurement using a LCR meter, and (d-e) Estimated and measured resonance frequencies.

[1] A. K. Das and B. G. Fernandes, "Synthesis of an Equivalent π-model of Two-winding Transformer and Resonance Frequency Estimation Using Lumped Circuit Parameters," ECCE 2019, pp. 3025-3032.

Thank you